1950

An experimental determination of the low-level characteristics of IN23B crystals.

Rushlow, Bruce Albert
Johns Hopkins University

AN EXPERIMENTAL
DETERMINATION OF THE
LOW-LEVEL CHARACTERISTICS
OF IN23B CRYSTALS

BY

BRUCE ALBERT RUSHLOW

AN EXPERIMENTAL DETERMINATION

OF THE LOW-LEVEL CHARACTERISTICS OF

 IN23B CRYSTALS

by

Bruce Albert Rushlow

AN ESSAY

SUBMITTED TO THE ADVISORY BOARD OF THE

SCHOOL OF ENGINEERING, THE JOHNS HOPKINS UNIVERSITY

IN CONFORMITY WITH THE REQUIREMENTS FOR

THE DEGREE OF MASTER OF SCIENCE IN ENGINEERING

Baltimore

1950

ACKNOWLEDGEMENT

The author wishes to express his sincere appreciation to Dr. J. V. Lebacqz for his suggestions and aid throughout the course of this work, and to Dr. F. Hamburger, Jr. for his suggestions and aid in the writing of this paper.

The author wishes also to express his sincere thanks to Mr. George Bush of the Johns Hopkins University Applied Physics Laboratory for his guidance and aid during the initial phases of this work.

TABLE OF CONTENTS

LIST OF TABLES AND FIGURES

I

INTRODUCTION

The development of microwave electronics equipment during World War II returned the crystal rectifier to a place of prominence in the field of electronics. There is at present no component in the development stage that will lessen the crystal rectifier's importance.

Many types of crystal rectifiers have been developed in the past ten years. Among these the high sensitivity, low burnout IN23B is probably the most widely used. Though used primarily as a mixer crystal, it is also used as a low-level detector with good results. However, a search for specific information in the low-level video characteristics revealed very little useable information.

In this paper a summary of the general theory of low-level video crystals is given, followed by the experimental determination of the low-level video characteristics for the IN23B crystal. The experimental results are summarized, and recommendations as to the proper use of these crystals in voltage and power amplification units are given.

OUTLINE OF THEORY OF CRYSTAL RECTIFIERS

The Barrier-Layer Rectification Principle (2, 27, and 8)*

A typical crystal rectifier unit is shown in Figure 1. Figure 2 gives the conventional polarity of crystal cartridges. The unit depends for its action on the electrical characteristics of the semiconductor.

A semiconductor is a substance which offers low impedance to the flow of current in one direction and high impedance to the flow of current in the opposite direction. Rectification results from the presence, in the semiconductor adjacent to the metal whisker contact, of a potential barrier or hill which current carriers, electrons or holes, must overcome in order to flow across the metal-semiconductor junction. The low impedance direction is that in which the carriers flow from the semiconductor to the metal whisker.

If a voltage is applied to the rectifier in the low impedance or forward direction it tends to reduce the potential barrier and thus lower the crystal impedance. If a voltage is applied in the reverse direction it tends to increase the barrier layer and thus increase the impedance to current flow. A typical voltage-current curve resulting from this action is shown in Figure 3.

---

* Paranthesized numbers refer to the bibliography.

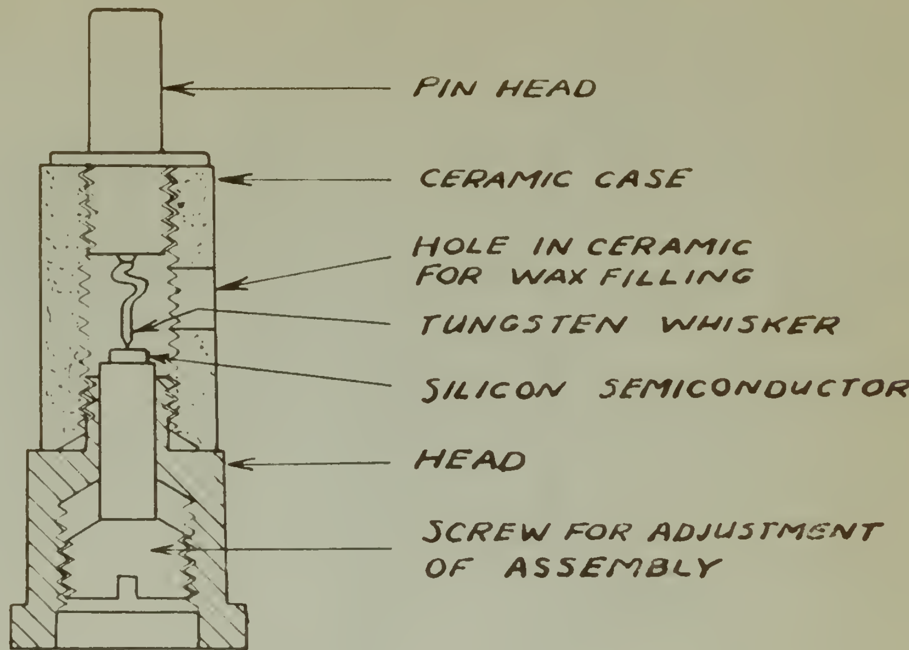

FIGURE 1. - Ceramic Cartridge

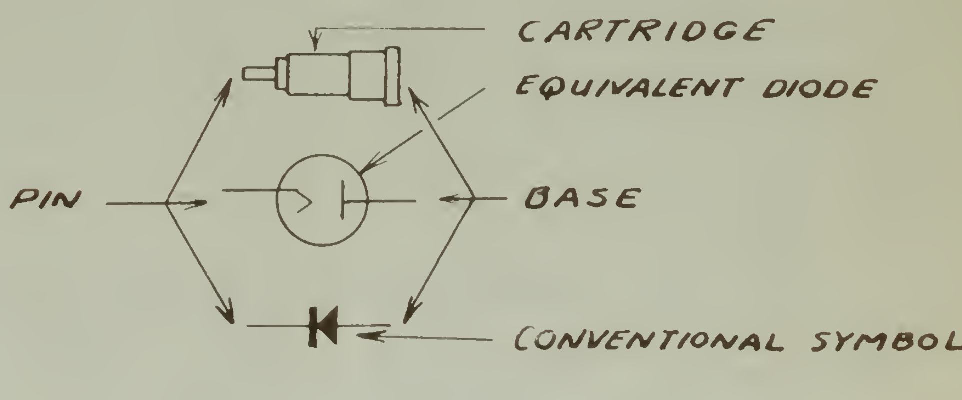

FIGURE 2. - Cartridge Polarity

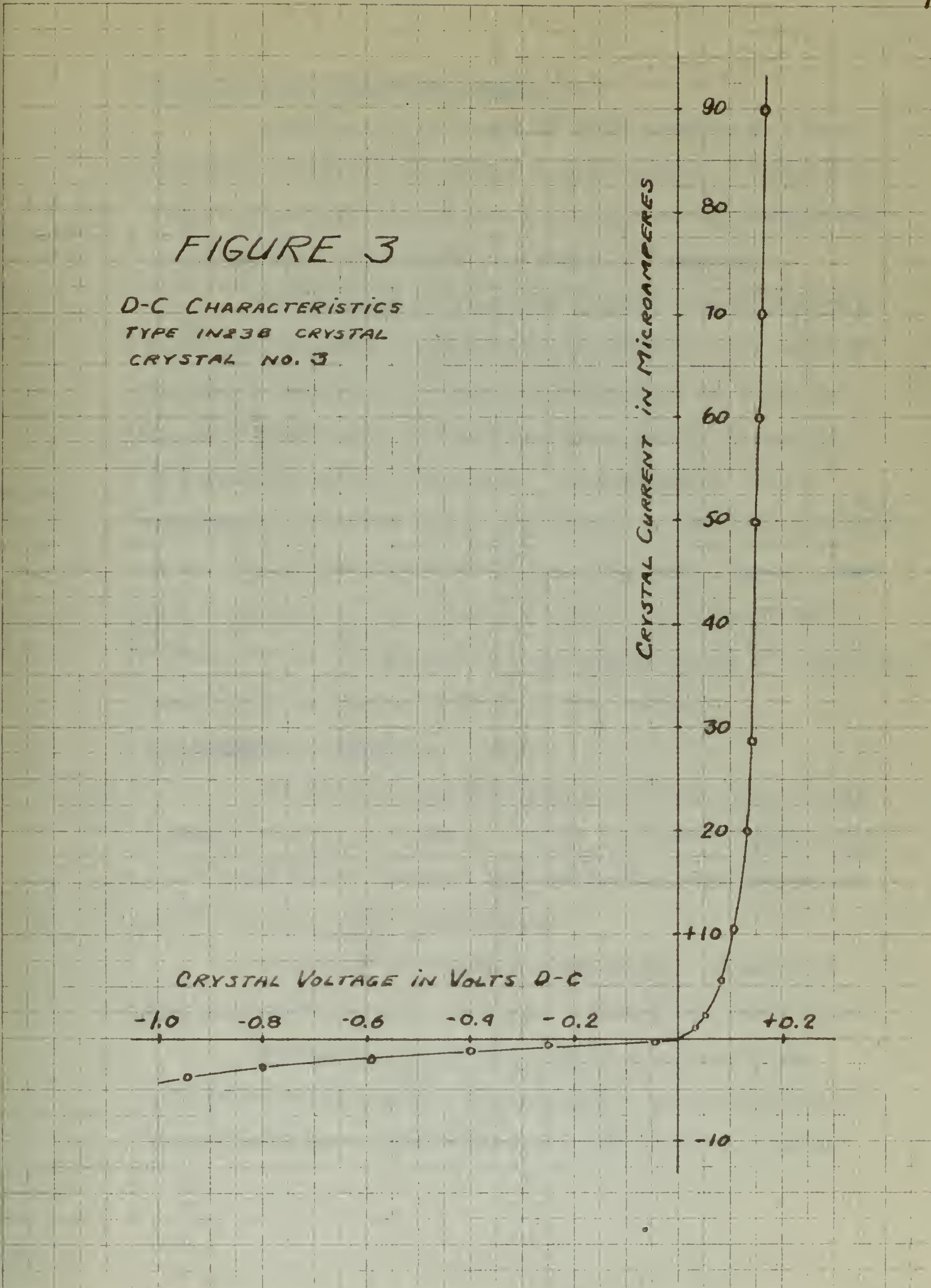
FIGURE 3
D-C CHARACTERISTICS
TYPE IN23B CRYSTAL
CRYSTAL NO. 3
CRYSTAL CURRENT IN MICROAMPERES
CRYSTAL VOLTAGE IN VOLTS D-C
90
80
70
60
50
40
30
20
+10
-10
-1.0
-0.8
-0.6
-0.4
-0.2
+0.2

The Crystal as a Square-Law Detector (1, 2)

Detecting devices depend for their operation on a non-linearity of their voltage-current characteristics. A detector is called a square-law detector when its voltage-current characteristic at the operating point can be approximated by a parabola.

The output of the square-law detector will be composed of a d-c component and an a-c component proportional to the square of the input voltage for each frequency component of the input plus the sum and difference frequencies of every possible combination of frequencies in the input signal. The magnitude of the a-c component in the output will be proportional to the second derivative of the characteristic curve at the operating point. Maximum output will be obtained when the operating point is the point of maximum curvature of the voltage-current characteristic curve. The operating point may be adjusted by means of the bias voltage.

The Equivalent Circuit (2, 5, and 6)

The generally accepted equivalent circuit of the crystal rectifier is shown in Figure 4. This is the simplest possible form and is based on the assumption that the whisker makes single-point contact with the silicon semiconductor.

The barrier resistance R is non-linear. It decreases with application of forward bias, and increases with reverse bias.

The spreading resistance r is the resistance of the semiconductor-metal contact, and is caused by the constriction of current flow lines in the semiconductor near the whisker contact

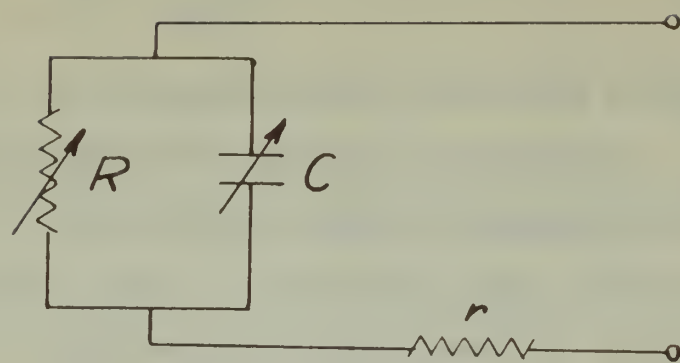

FIGURE 4. - EQUIVALENT CIRCUIT OF A CRYSTAL RECTIFIER

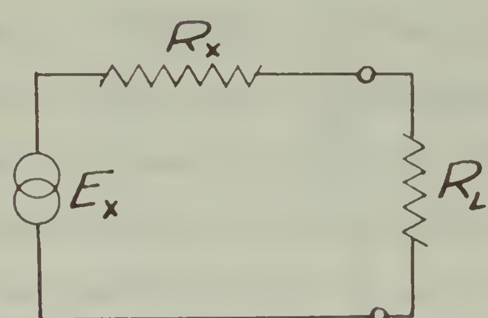

FIGURE 5. - VOLTAGE GENERATOR CIRCUIT OF A VIDEO CRYSTAL

point. If the contact is considered to be circular (8), r is given by

$$r = \frac{1}{4\sigma a} \qquad \text{(ohms)} \qquad (1)$$

where σ is the semiconductor conductivity in $(\text{ohm-cm})^{-1}$ and a is the radius of the contact in centimeters.*

The non-linear barrier capacitance C is a result of the storage of charge in the boundary layer. The value of C at zero bias is approximately 10 micromicrofarad. It is relatively independent of variations in applied voltage (21). At high frequencies C acts as a by-pass to R. At video frequencies C plays no important part in the rectification phenomenon.

When a crystal is operating as a square-law detector it is convenient to represent it as a four terminal network in which the video and microwave terminals are considered isolated from each other (7). Since the microwave energy source is not affected by the output load, it is possible to represent the crystal as a voltage generator of output voltage E_x proportional to the input power, and an internal resistance of $R_x = R + r$. This is shown in Figure 5. E_x and R_x are obviously both functions of crystal bias, and thus this voltage generator concept is good only for the bias specified. The load is connected as shown in the figure.

---

* See Appendix C of (2) for the spreading resistance of an elliptical contact. (8) discusses the knife edge contact of the British "Red Dot" crystal.

Low-Level Properties

From Figure 4 it is seen that the output impedance of the crystal is

$$Z = r + \frac{1}{\frac{1}{R} + j\omega C} \qquad \text{(ohms)} \qquad (2)$$

At video frequencies the $j\omega C$ term is small compared to $\frac{1}{R}$. Thus the video impedance becomes a pure resistance and is given by

$$Z = R_x = R + r \qquad \text{(ohms)} \qquad (3)$$

The current sensitivity of a crystal β is defined as the ratio of the short circuit rectified current to the absorbed microwave power,

$$\beta = \frac{i_s}{P} \qquad \frac{\text{(microamperes)}}{\text{(microwatt)}} \qquad (4)$$

Beringer (7), and Lawson et al (14) have shown that the variation of β with bias may be expressed as

$$\beta = \beta_o \cdot \frac{1}{1 + \frac{\omega^2 C^2 r R^2}{R + r}} \qquad (5)$$

where R, r, and C are as previously defined, and β_o is the current sensitivity at zero bias.

The crystal detector is a noise generator as well as a microwave converter. Beringer (7) has derived an expression for the output signal-to-noise voltage ratio of a crystal-video receiver in which he defines a quantity called the Figure of Merit, M.

The output signal-to-noise voltage ratio is given by

$$\frac{E_s}{E_N} = \frac{\beta P R_x}{\sqrt{4kTB(R_x t + R_a)}} \tag{6}$$

E_s Signal voltage output
E_n Noise voltage output
R_a Equivalent noise resistance of the receiver, set by JAN specifications at 1,200 ohms.
k Boltzmann's constant, 1.38×10^{-23} Joules/°K
T Temperature of R_a in degrees Kelvin
B Noise bandwidth of receiver in cps.
t Crystal noise temperature*

From Equation 6 all the crystal parameters are lumped together by Beringer and called the Figure of Merit,

$$M = \frac{\beta R_x}{\sqrt{R_x t + R_a}} \tag{7}$$

Smith (25) has shown that t is approximately equal to 1.0 within the bias region used in the following experiments. The value of 1.0 will be used throughout the paper.

From Equation 6 it is seen that for a given receiver operating at a constant temperature, and for a specified signal-to-noise voltage output ratio, M is inversely proportional to P.

$$M = \frac{K}{P} \tag{8}$$

---

* By definition t is the ratio of the available noise power output of the crystal to that of a resistor at room temperature. Though it is not a temperature, the term "noise temperature" is commonly accepted and widely used.

TEST EQUIPMENT

In Figure 6 is shown a block diagram of the test equipment.

The microwave generator is a calibrated output TS-13/AP, operated square-wave modulated.

The audio amplifier is a high gain, wide and narrow band TAA-16EA*. It was operated narrow band and amplified only the fundamental of the crystal output pulse. The input transformer was by-passed, and the output from the crystal loading circuit placed on the input gain control. This input circuit arrangement gave an input impedance to the amplifier of 0.5 megohms. The 6H6 output rectifier tube was removed and the signal normally applied to its plate was measured by the Hewlett-Packard Model 400A voltmeter.

In determination of the Figure of Merit the TAA-16EA was replaced by a Ballantine voltmeter Model 300 whose input resistance is 0.5 megohms. Also a DuMont Model 208-B oscilloscope was used as an output indicator in place of the Hewlett-Packard voltmeter.

The circuit used to bias and load the crystal is shown in detail in Figure 7. To keep noise pick-up to a minimum it was necessary to place all components enclosed by the dashed line in Figure 7 marked chassis in a completely enclosed metal chassis.

---

* A circuit diagram of this piece of equipment may be found in "Technique of Microwave Measurements", Montgomery, McGraw-Hill Book Company, p 501.

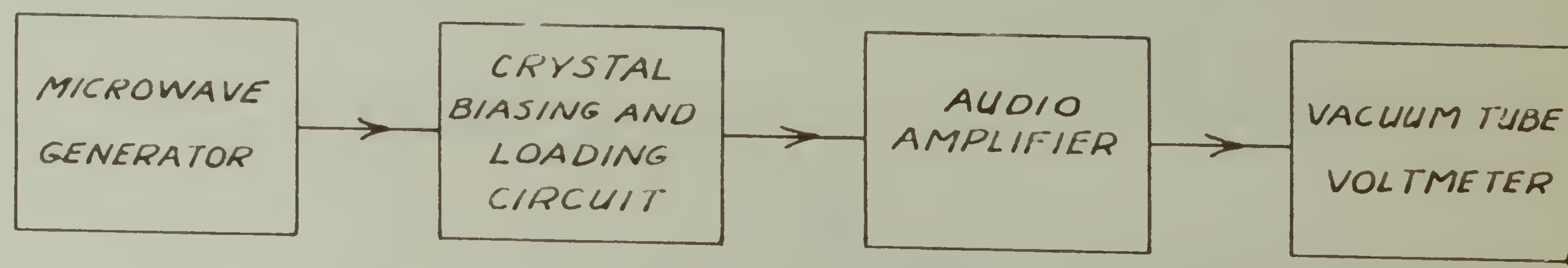

FIGURE 6.

Block Diagram of Test Equipment

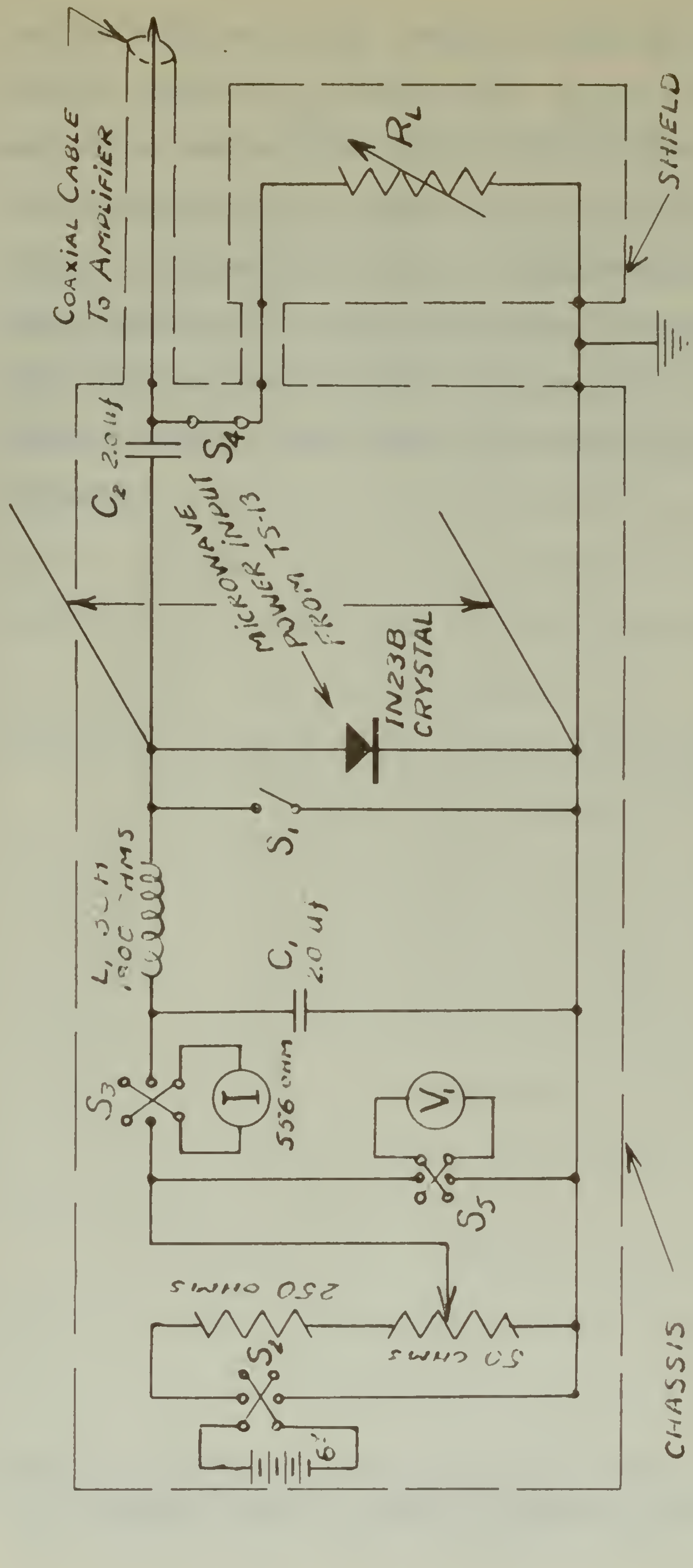

FIGURE 7.

Biasing and Loading Circuit

The load resistance R_L had a built-in shield and was connected to the metal chassis by a coaxial cable. R_L was a non-inductively wound decade resistance box with a maximum resistance of 100,000 ohms. The microwave power was carried from the TS-13/AP by means of standard 3 cm. band waveguide to a variable-tuned 3 cm band crystal holder mounted on the side of the biasing circuit chassis*. The output terminal of the crystal holder was inside the chassis. The effective microwave input terminals are shown by the diagonal lines in Figure 6.

* For detailed drawing of crystal holder see page 353 of (2).

IV

TEST PROCEDURE AND RESULTS

Since it is possible to represent the video crystal as a voltage generator with an internal resistance, it is apparent that maximum power transfer to the load resistance will occur when R_x equals R_L provided E_x remains constant. The determination of the variation of R_x with power level and bias is based on this maximum power transfer principle. Five crystals were chosen at random from the available supply so that a measure of the variation to be expected from crystal to crystal could be determined*. All crystals were of Sylvania design and manufacture.

Variation of Crystal Resistance With Microwave Power Level

The first experiment was designed to determine the variation of R_x with variation in the microwave power input to the crystal. A bias current of 10 microamperes was put through the crystal and the load varied for a constant input power of 30dbm (decibels below a milliwatt). The output voltage shown on the Hewlett-Packard voltmeter was recorded. The above procedure was repeated for input power levels of 40dbm and 45dbm. The results of all three power levels are plotted in Figure 7.

To determine R_x it is necessary to find that value of R_L which makes the power transferred to the load a maximum. This is done by determining the point at which a line of constant power

---

* For identification purposes the crystals used were assigned numbers. These numbers appear on the curves throughout the paper.

is tangent to the desired curve. The point of tangency will be at that value of R_L for which the power in the load is a maximum. A line of constant power is shown in the figure for reference. The vertical marks on each curve show the points of tangency. R_L at this point is equal to R_x for the bias current used in the experiment.

From Figure 8 it is seen that the variation of crystal resistance is negligible for power input between 0.03 and 1.0 microwatts (45dbm and 30dbm). The remainder of the experiments have been conducted at the 40dbm level and the results are considered valid for the entire microwatt region (50dbm to 20dbm).

Variation of Crystal Resistance With Bias

The curves of Figures 9, 10 and 11 were obtained for bias currents of 0.0, 5.0 and 10.0 microamperes respectively by varying the crystal load resistance and recording the output voltage as read on the Hewlett-Packard voltmeter at constant power input. By determining the point of tangency of the line of constant power, we can as before get the value of R_x. The points of tangency are indicated by short vertical lines on the curves. The value of R_x is shown by vertical lines near the bottom of the Figures, the value being read on the R_L scale.

A second means of determining crystal resistance-bias characteristics is the halving method. If the open circuited voltage of Figure 5 is known and R_L is adjusted to give an output voltage of one half the open circuited voltage, application of Thevenin's Theorem shows that R_L is equal to R_x. Computations show that the maximum expected error in determination of R_x by

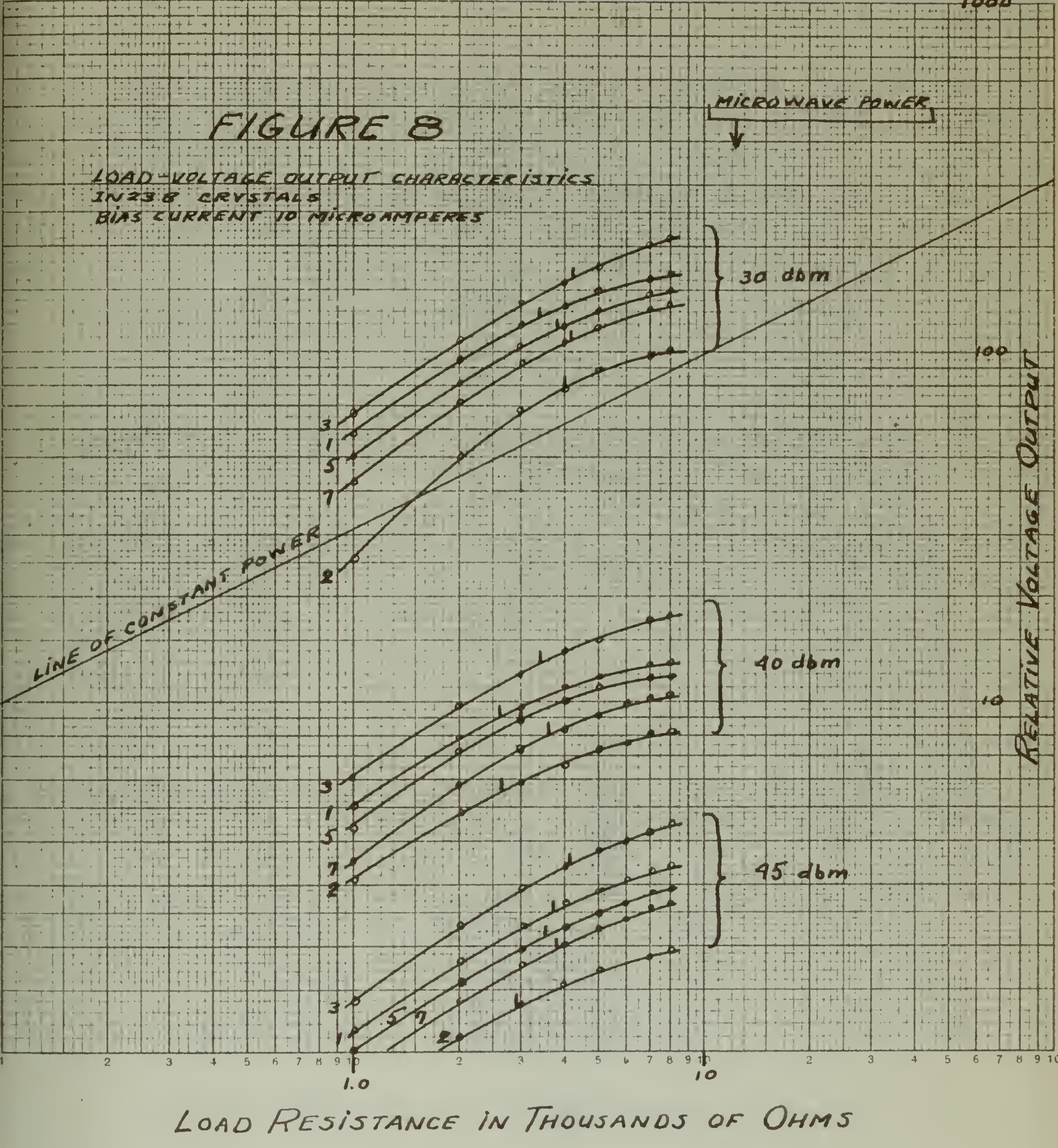
FIGURE 8
LOAD-VOLTAGE OUTPUT CHARACTERISTICS
1N23B CRYSTALS
BIAS CURRENT 10 MICROAMPERES
MICROWAVE POWER
30 dbm
40 dbm
45 dbm
LINE OF CONSTANT POWER
1000
100
10
RELATIVE VOLTAGE OUTPUT
1.0
10
LOAD RESISTANCE IN THOUSANDS OF OHMS

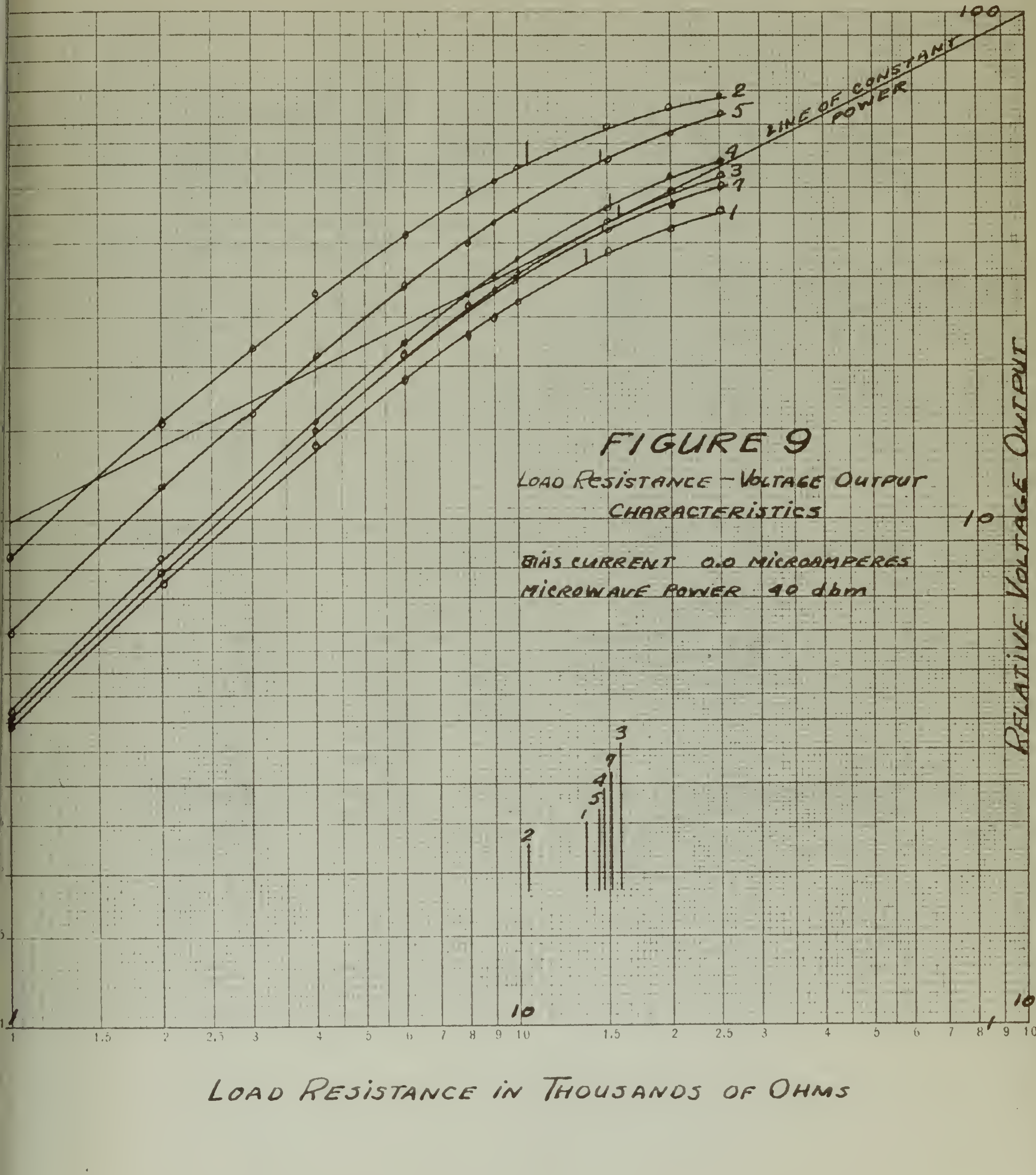
FIGURE 9
LOAD RESISTANCE - VOLTAGE OUTPUT
CHARACTERISTICS
BIAS CURRENT 0.0 MICROAMPERES
MICROWAVE POWER 40 dbm
LINE OF CONSTANT POWER
RELATIVE VOLTAGE OUTPUT
1
1.5
2
2.5
3
4
5
6
7
8
9
10
100
LOAD RESISTANCE IN THOUSANDS OF OHMS

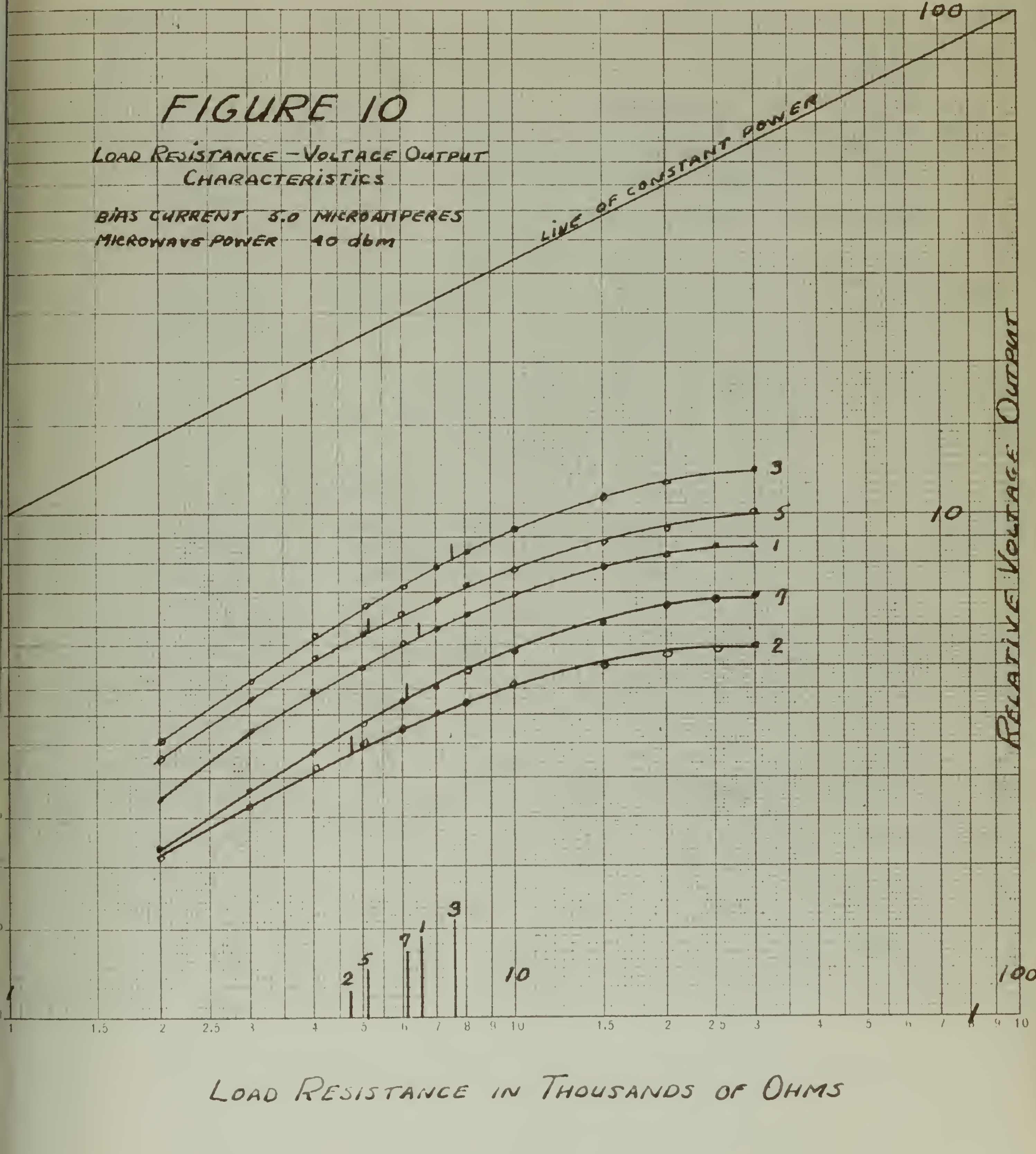
FIGURE 10
LOAD RESISTANCE – VOLTAGE OUTPUT CHARACTERISTICS
BIAS CURRENT 5.0 MICROAMPERES
MICROWAVE POWER 10 dbm
LINE OF CONSTANT POWER
RELATIVE VOLTAGE OUTPUT
LOAD RESISTANCE IN THOUSANDS OF OHMS
100
10
1
3
5
1
7
2
2
5
7
1
3
10
100
1.5
2
2.5
3
4
5
6
7
8
9
10
1.5
2
2.5
3
4
5
6
7
8
9
10

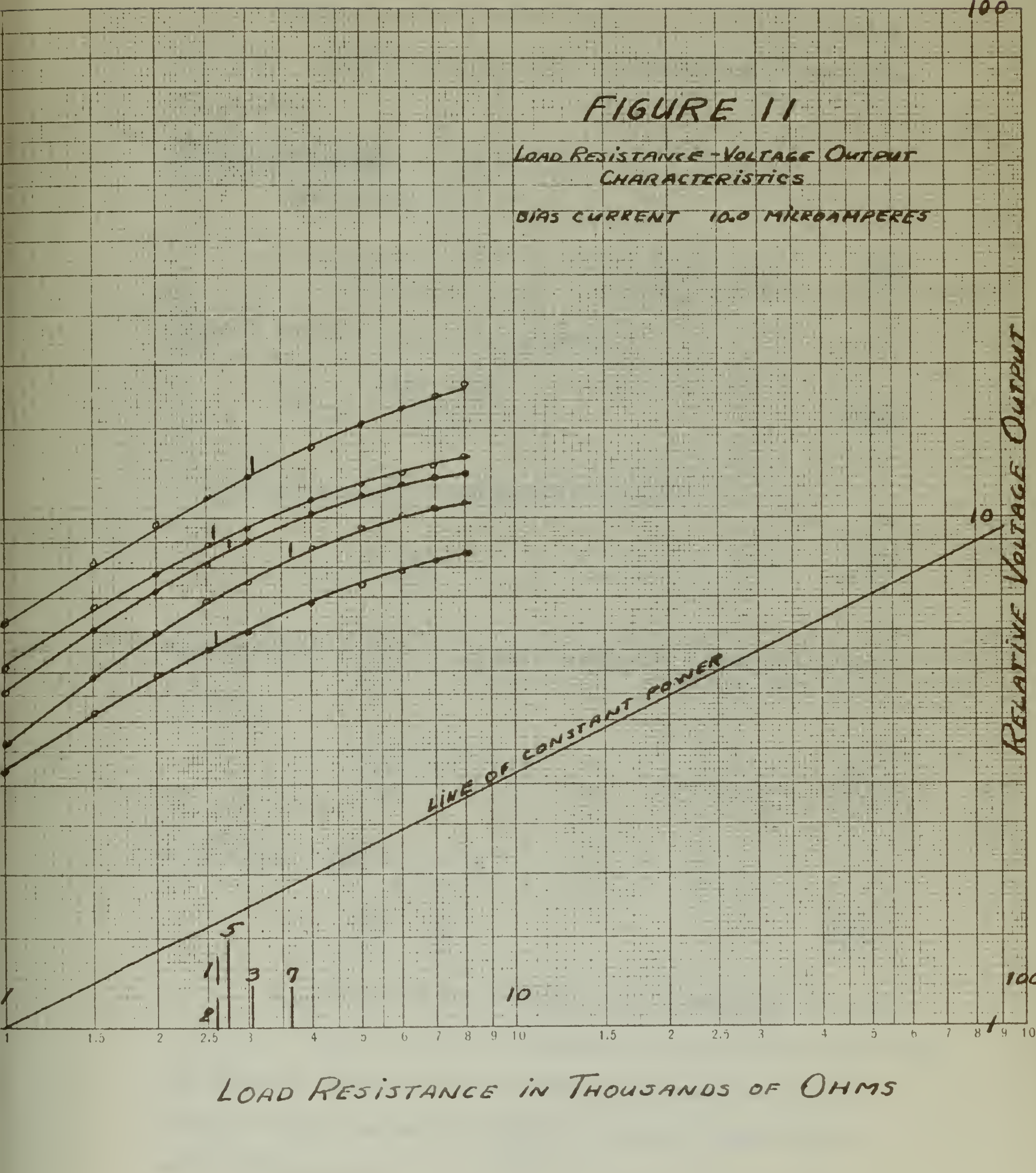
FIGURE 11
LOAD RESISTANCE - VOLTAGE OUTPUT CHARACTERISTICS
BIAS CURRENT 10.0 MICROAMPERES
LINE OF CONSTANT POWER
RELATIVE VOLTAGE OUTPUT
LOAD RESISTANCE IN THOUSANDS OF OHMS

This halving method is 3 percent and is due to the input resistance of the amplifier not being infinity, but 500,000 ohms. The results of this procedure are tabulated in Table I. Using this data the curves for crystals number 3 and 5 were plotted and are shown in Figure 12.

<u>Current Sensitivity</u>

From Equation 4,

$$i_s = \beta P \tag{9}$$

Refering to Figure 5, it is seen that,

$$E_x = \frac{(R_x + R_L)}{R_L} V_L \tag{10}$$

If R_L is set equal to zero in Figure 5, then,

$$i_s = \frac{E_x}{R_L} \tag{11}$$

Equating Equations 9 and 11, and substituting Equation 10 for E_x gives,

$$\beta = \frac{(R_x + R_L)}{R_x R_L P} V_L \tag{12}$$

If R_L is set equal to R_x, then

$$\beta = \left(\frac{2}{P}\right) \cdot \frac{V_L}{R_L} \tag{13}$$

V_L and R_L, for the condition that R_L equal R_x, are given in Table I. Using this data and Equation 13, the curves in Figure 13 were plotted. Since R_x is not a function of power level in the microwatt region the constant $\left(\frac{2}{P}\right)$ acts only as a linear scale factor for the curves.

TABLE I

CRYSTAL RESISTANCE

	CRYSTAL No. 1		CRYSTAL No. 2		CRYSTAL No. 3		CRYSTAL No. 5		CRYSTAL No. 7	
I	E_L	R_x	E_L	R_x	E_L	R_x	E_L	R_x	E_L	R_x
0.0	5.40	10.0	4.60	9.30	3.25	11.1	5.85	10.8	3.90	11.6
2.5	9.75	4.80	5.25	5.30	11.0	8.00	8.50	6.20	8.00	7.00
5.0	9.75	3.56	5.25	3.95	11.2	5.50	8.40	4.20	8.00	4.70
7.5	9.50	3.25	5.20	3.14	10.8	4.40	8.10	3.20	7.70	3.54
10.0	9.10	2.60	5.10	2.54	10.5	3.20	7.50	2.40	7.40	2.87
20.0	7.70	1.41	4.65	2.27	9.20	1.65	6.50	1.45	6.20	1.64
30.0	6.60	.94	4.25	1.05	7.50	1.10	5.70	.99	5.40	1.17
40.0	6.00	.78	3.92	.82	6.70	.93	5.10	.86	5.00	1.03
50.0	5.30	.64	3.70	.70	5.80	.75	4.60	.73	4.55	.83
60.0	5.00	.59	3.45	.58	5.20	.66	4.15	.63	4.10	.71
70.0	4.55	.53	3.20	.51	4.60	.58	3.70	.55	3.70	.62
80.0	4.10	.46	3.10	.49	4.30	.57	3.35	.48	3.35	.55
90.0	3.80	.43	2.85	.42	3.90	.52	3.10	.44	3.10	.51
100.0	3.60	.41	2.70	.40	3.70	.50	3.00	.43	2.90	.49

I = BIAS CURRENT IN MICROAMPERES

$R_x = R_L$ = CRYSTAL LOAD RESISTANCE AT $E_L = \frac{1}{2} E$ OPEN CIRCUIT

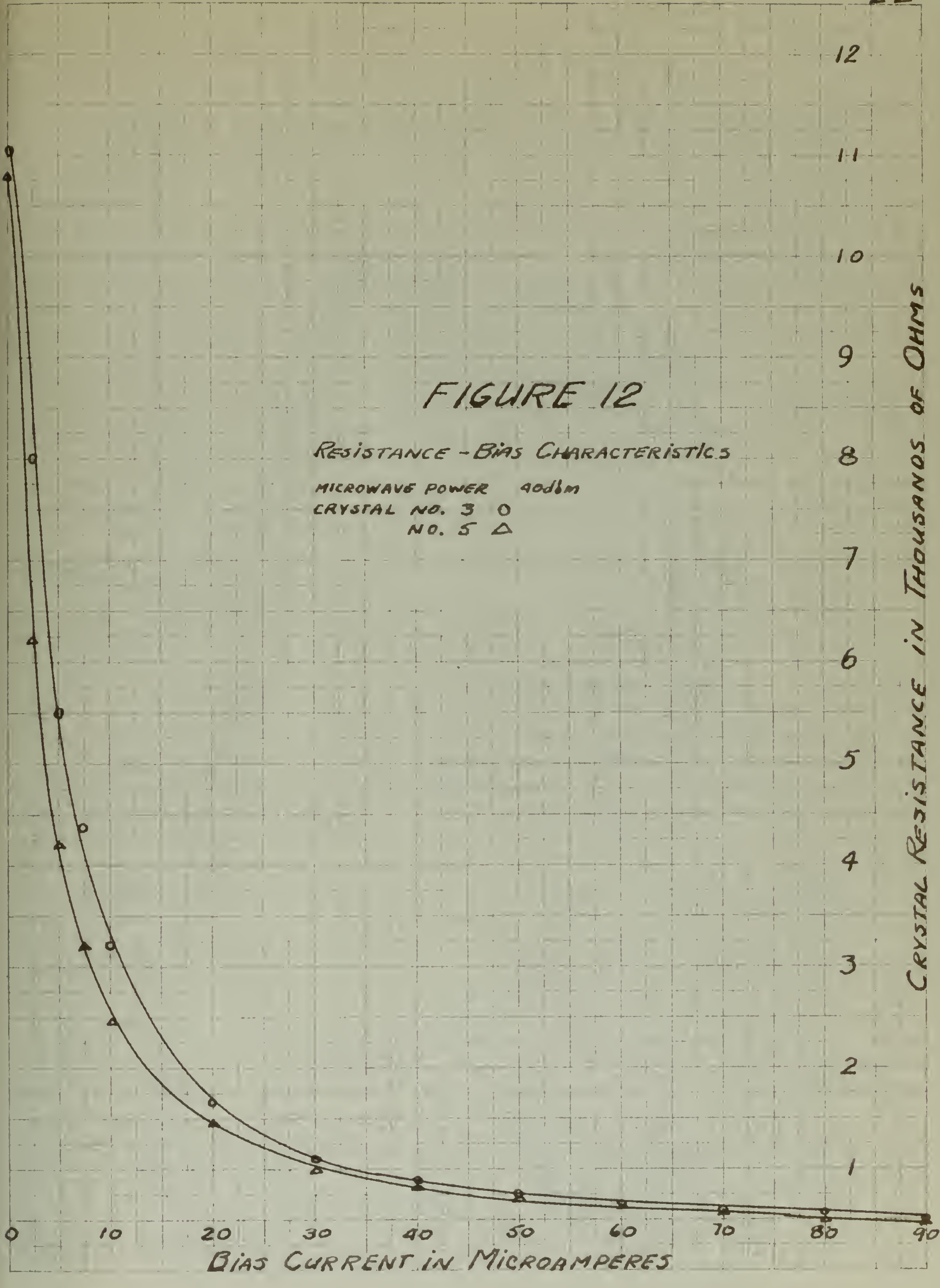
FIGURE 12
RESISTANCE - BIAS CHARACTERISTICS
MICROWAVE POWER 40dbm
CRYSTAL NO. 3 O
NO. 5 △
0
10
20
30
40
50
60
70
80
90
BIAS CURRENT IN MICROAMPERES
1
2
3
4
5
6
7
8
9
10
11
12
CRYSTAL RESISTANCE IN THOUSANDS OF OHMS

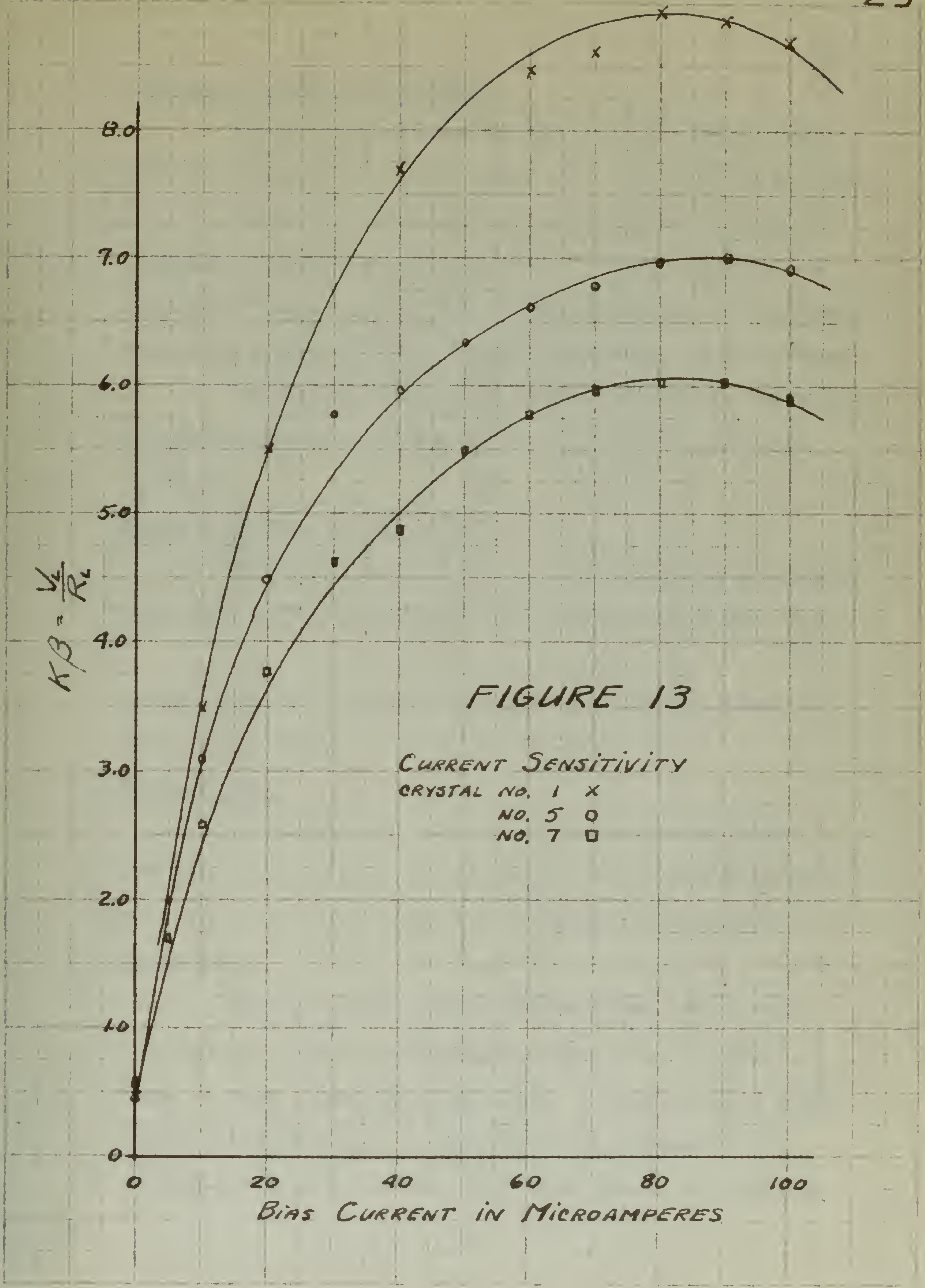

8.0
7.0
6.0
5.0
4.0
3.0
2.0
1.0
0
0
20
40
60
80
100
$K\beta = \frac{V_c}{R_c}$
Bias Current in Microamperes
Current Sensitivity
Crystal No. 1 x
No. 5 o
No. 7 □

FIGURE 13

Variation of Crystal Output Voltage

Crystal output voltage was investigated in three manners: 1) by the variation of the bias current with the load as a parameter, 2) by the variation of bias with the power input to the crystal as a parameter, the load being kept constant at 2,000 ohms, 3) by the variation of the power input with the bias being taken as a parameter. The results of these tests are shown in Figures 14, 15, 16 and 17.

Variation of crystal output voltage for different crystals was determined as a function of bias. The results are shown in Figure 18.

Variation of Crystal Power Output

The data given in Table I is for the condition of maximum power transfer from the crystal to the load. From this data $\frac{(E_o)^2}{R_L}$ was calculated and the resulting maximum power transfer curve is shown in Figure 19.

Figure of Merit

Two methods were used to determine the variation of M with bias. The first was by substituting into Equation 7, the data available in Table I and Figure 13. The results are given in Figure 20.

The second method was by experimentation based on the fact that for a given signal-to-noise voltage output ratio the Figure of Merit is inversely proportional to the power input to the crystal (See Equation 8). To determine M the bias current was adjusted to the desired value and the power output of the TS-13AP

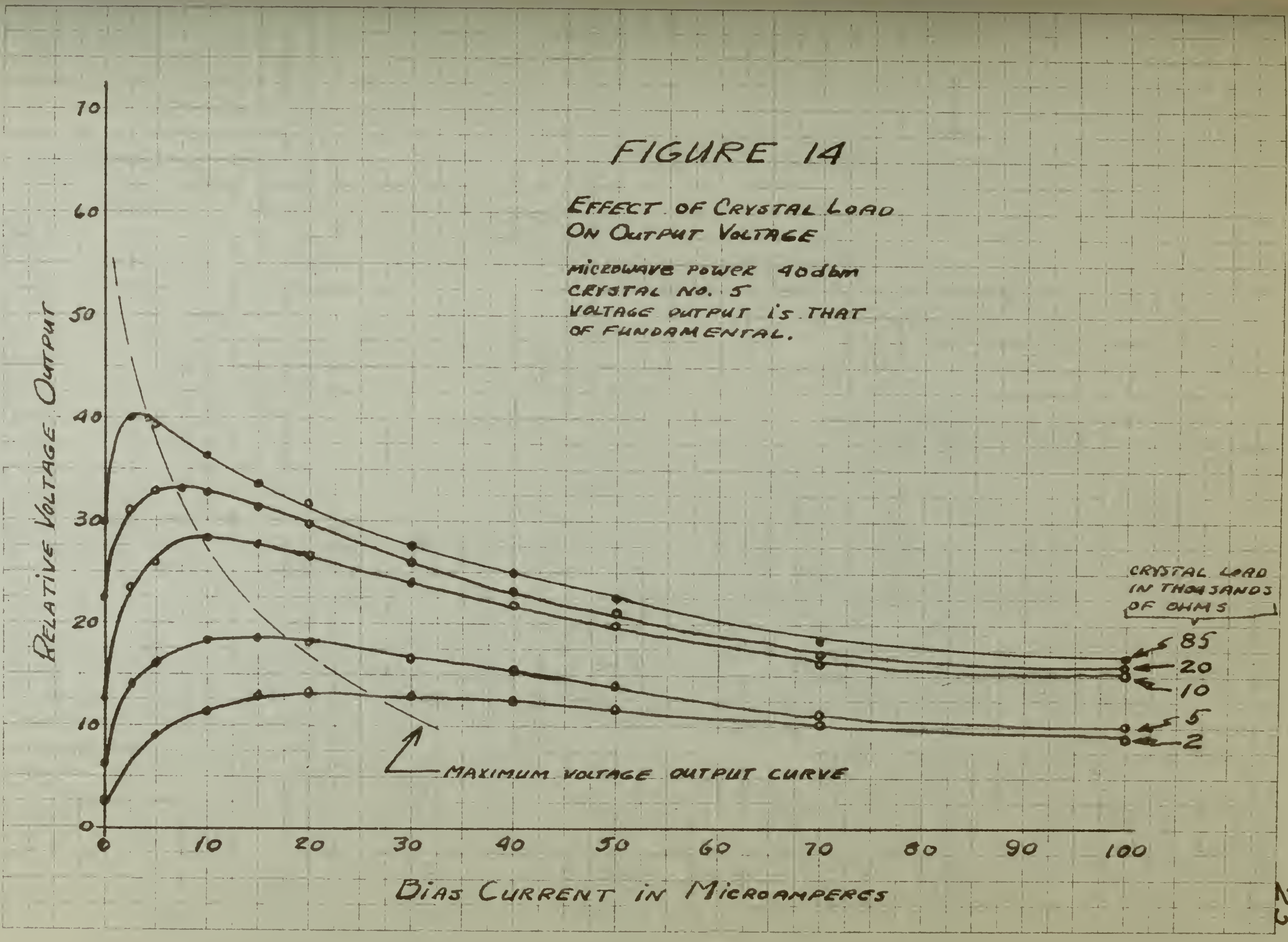
FIGURE 14
EFFECT OF CRYSTAL LOAD ON OUTPUT VOLTAGE
MICROWAVE POWER 40dbm
CRYSTAL NO. 5
VOLTAGE OUTPUT IS THAT OF FUNDAMENTAL.
RELATIVE VOLTAGE OUTPUT
BIAS CURRENT IN MICROAMPERES
MAXIMUM VOLTAGE OUTPUT CURVE
CRYSTAL LOAD IN THOUSANDS OF OHMS
85
20
10
5
2
0
10
20
30
40
50
60
70
80
90
100

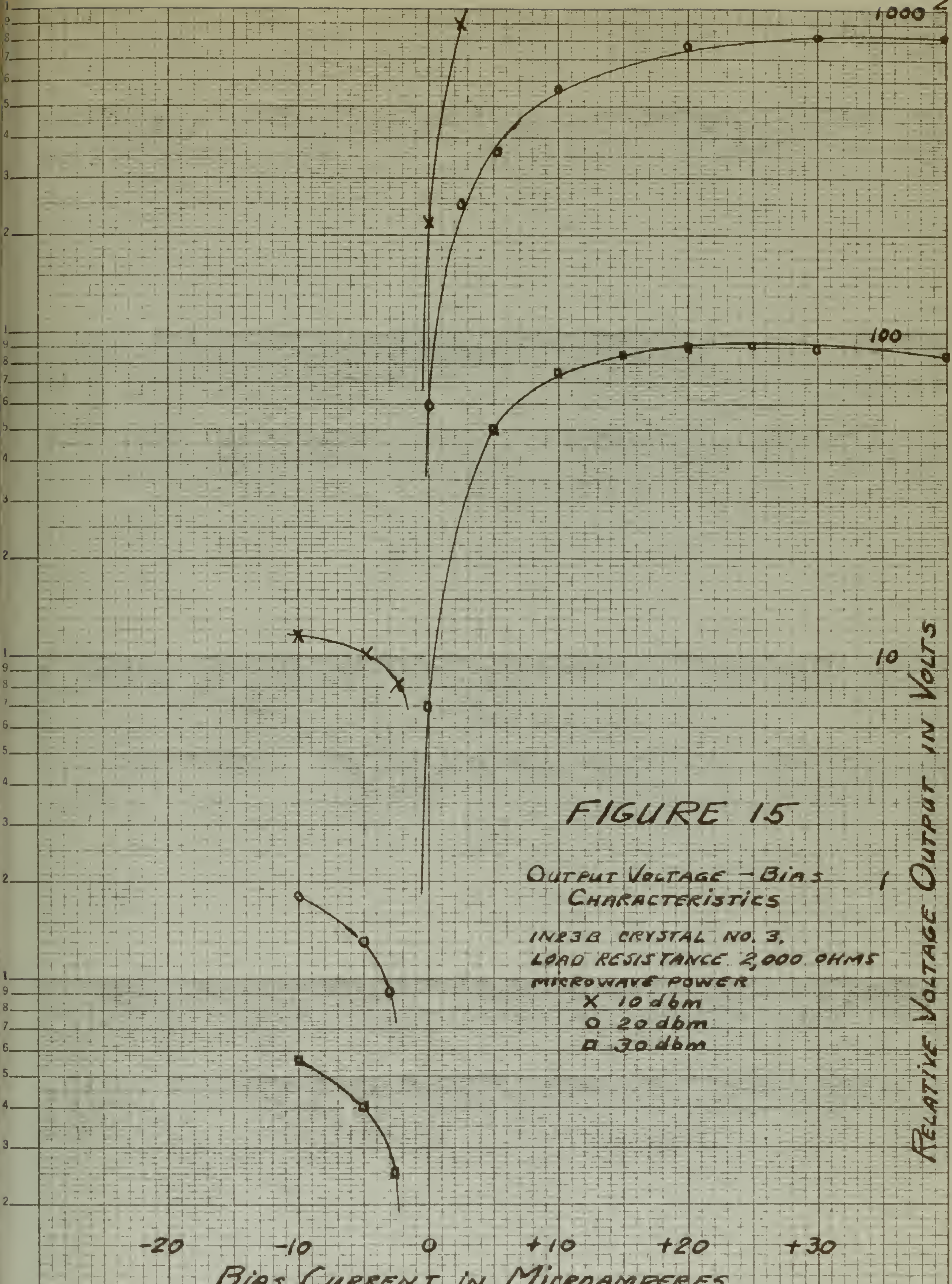
1000
100
10
1
-20
-10
0
+10
+20
+30
Bias Current in Microamperes
Relative Voltage Output in Volts
FIGURE 15
Output Voltage – Bias Characteristics
1N23B Crystal No. 3.
Load Resistance 2,000 Ohms
Microwave Power
X 10 dbm
O 20 dbm
□ 30 dbm

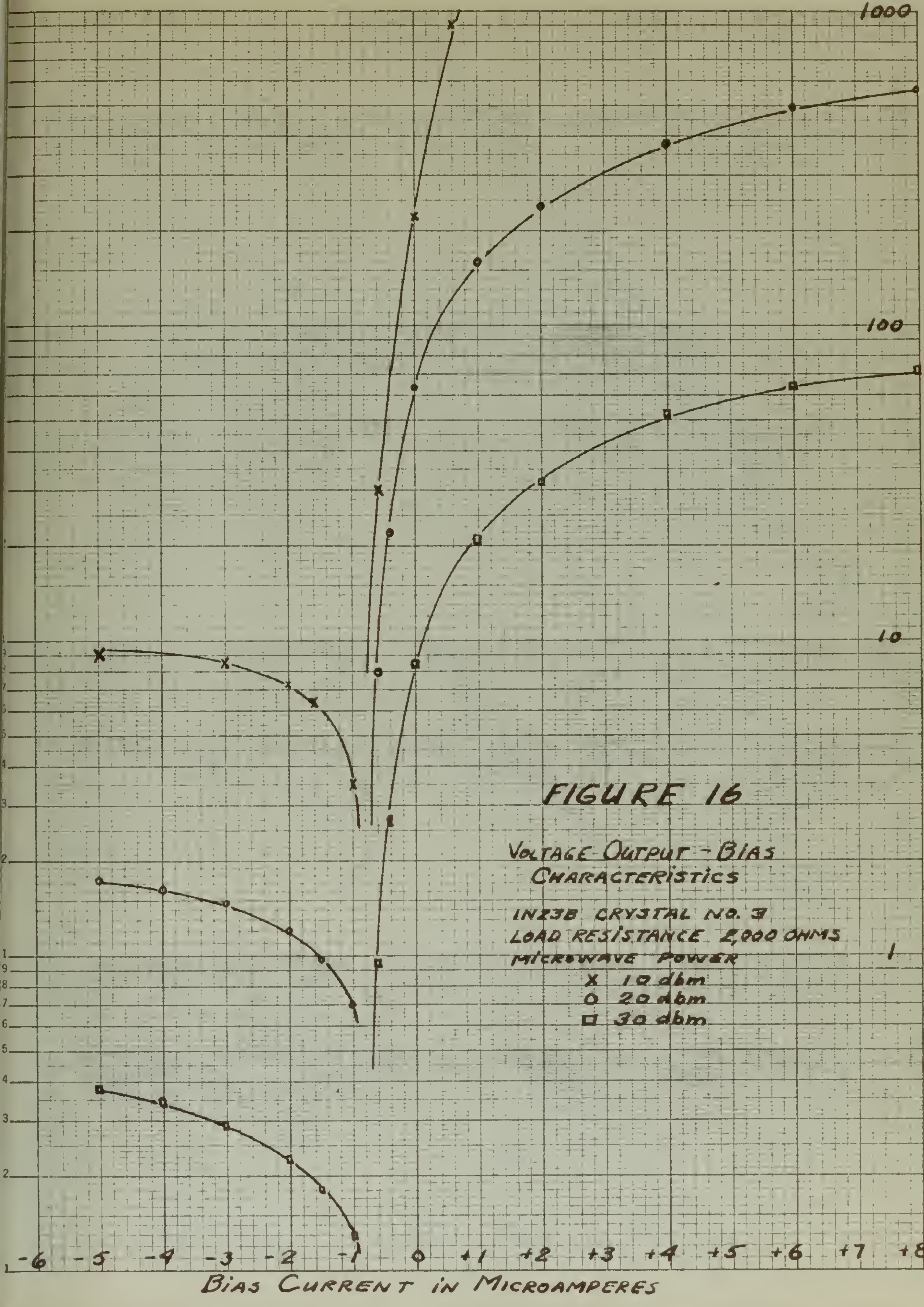
1000
100
10
1
-6 -5 -4 -3 -2 -1 0 +1 +2 +3 +4 +5 +6 +7 +8
RELATIVE VOLTAGE OUTPUT IN VOLTS
BIAS CURRENT IN MICROAMPERES
VOLTAGE OUTPUT - BIAS CHARACTERISTICS
IN23B CRYSTAL NO. 3
LOAD RESISTANCE 2,000 OHMS
MICROWAVE POWER
X 10 dbm
O 20 dbm
□ 30 dbm

FIGURE 16

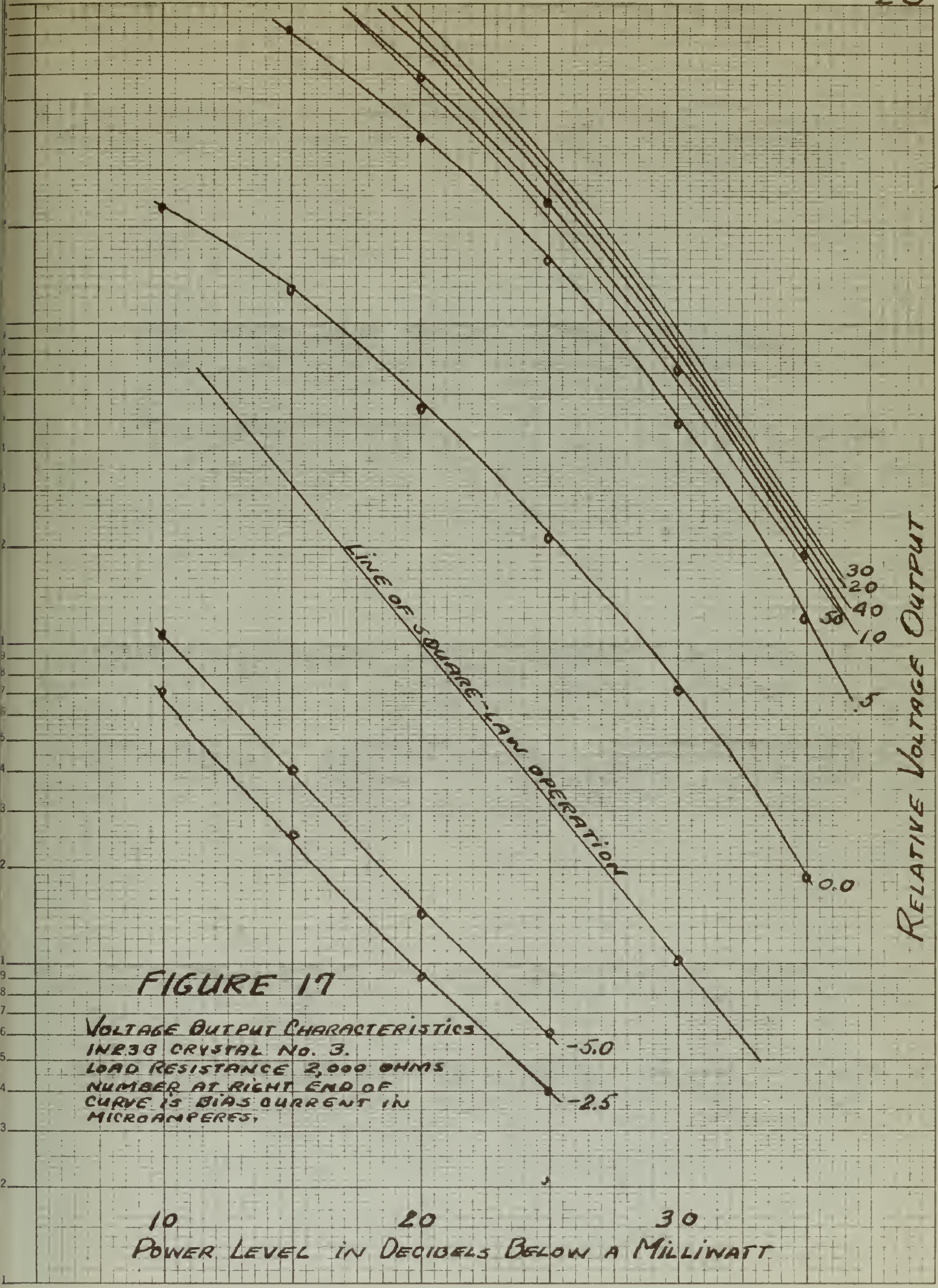

FIGURE 17

Voltage Output Characteristics
1N23B Crystal No. 3.
Load Resistance 2,000 ohms
Number at right end of curve is bias current in microamperes.

FIGURE 18

CRYSTAL OUTPUT CHARACTERISTICS
1N23B CRYSTALS
LOAD RESISTANCE 10,000 OHMS
MICROWAVE POWER 40 dbm

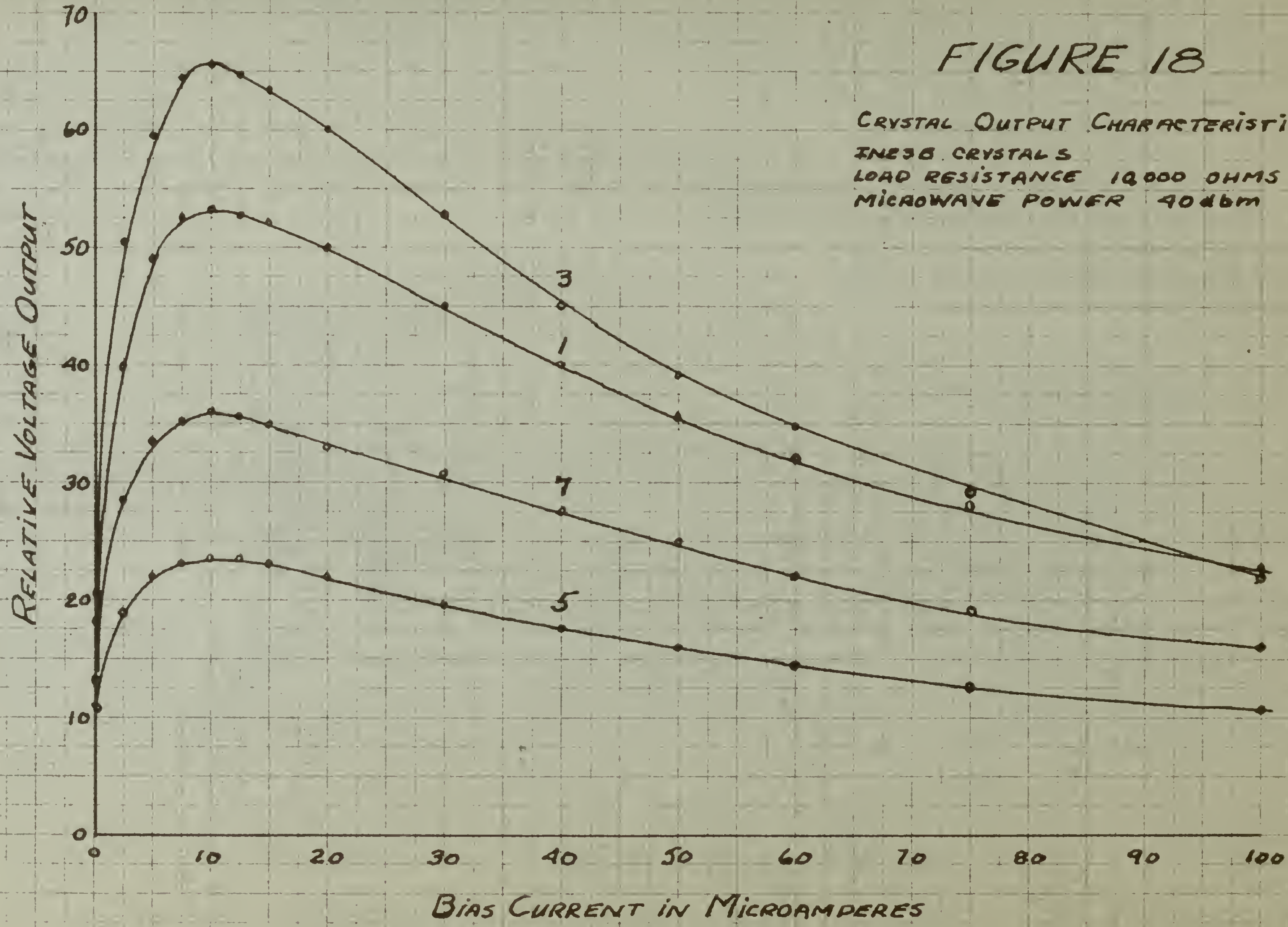

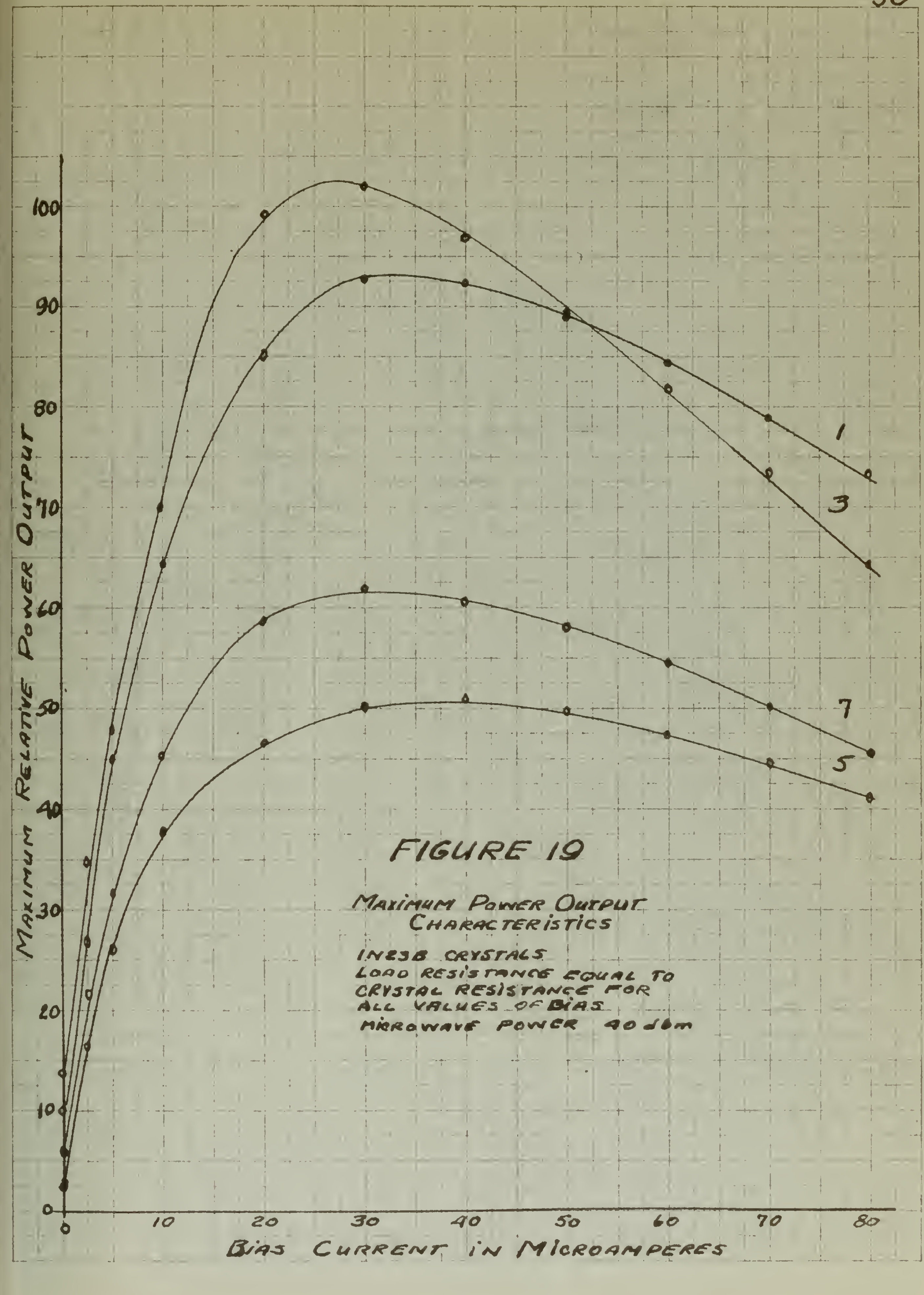

FIGURE 19

Maximum Power Output
Characteristics

1N23B crystals
Load resistance equal to
crystal resistance for
all values of bias
Microwave power 40 dbm

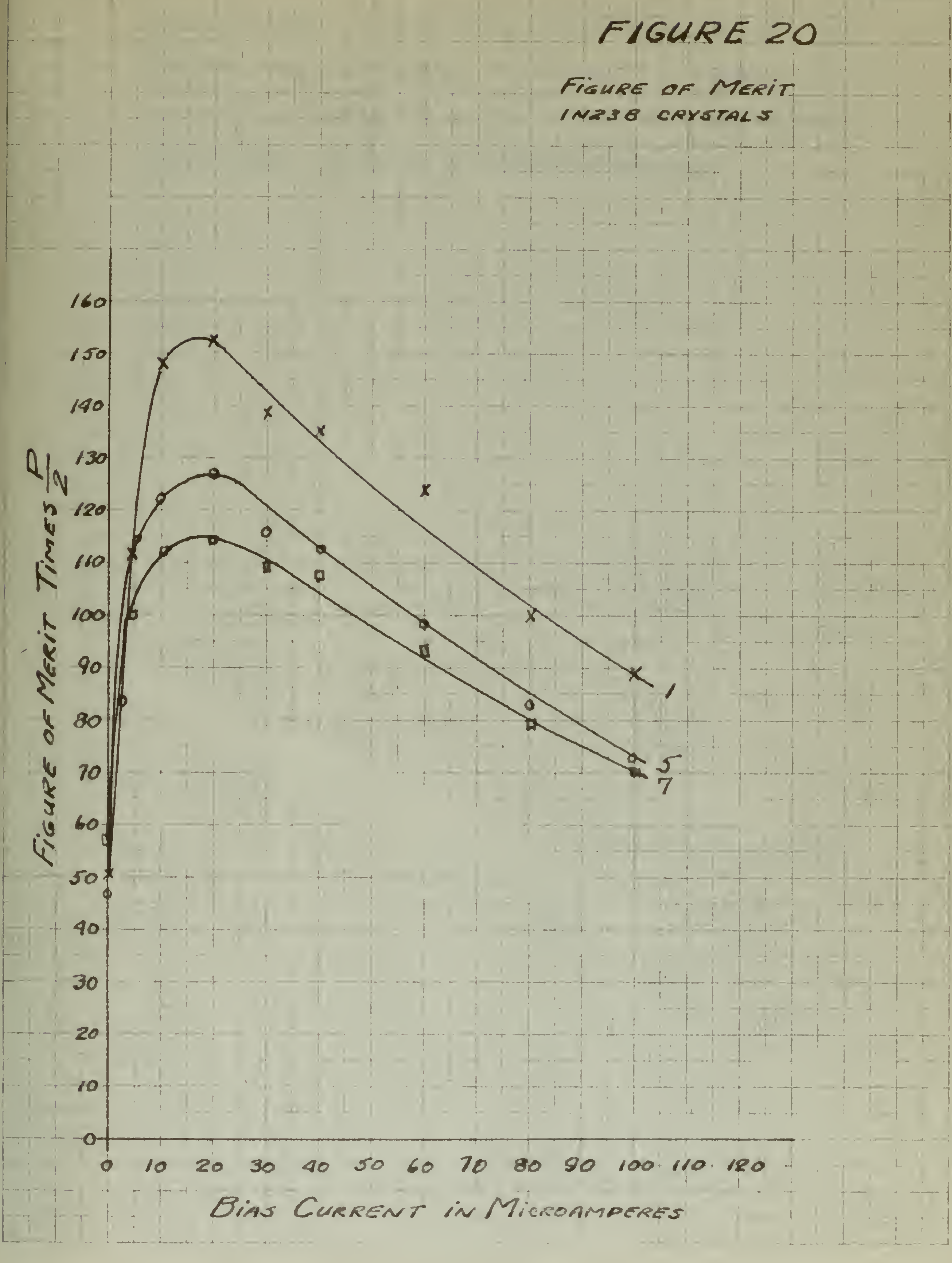
FIGURE 20
FIGURE OF MERIT
1N23B CRYSTALS
Figure of Merit Times $\frac{P}{2}$
Bias Current in Microamperes
0
10
20
30
40
50
60
70
80
90
100
110
120
130
140
150
160
1
5
7

decreased until a signal-to-noise voltage output ratio of 1 was observed on the oscilloscope. The inverse of this power is KW. The procedure was repeated for bias currents from zero to 100.0 microamperes. The results are plotted in Figure 21.

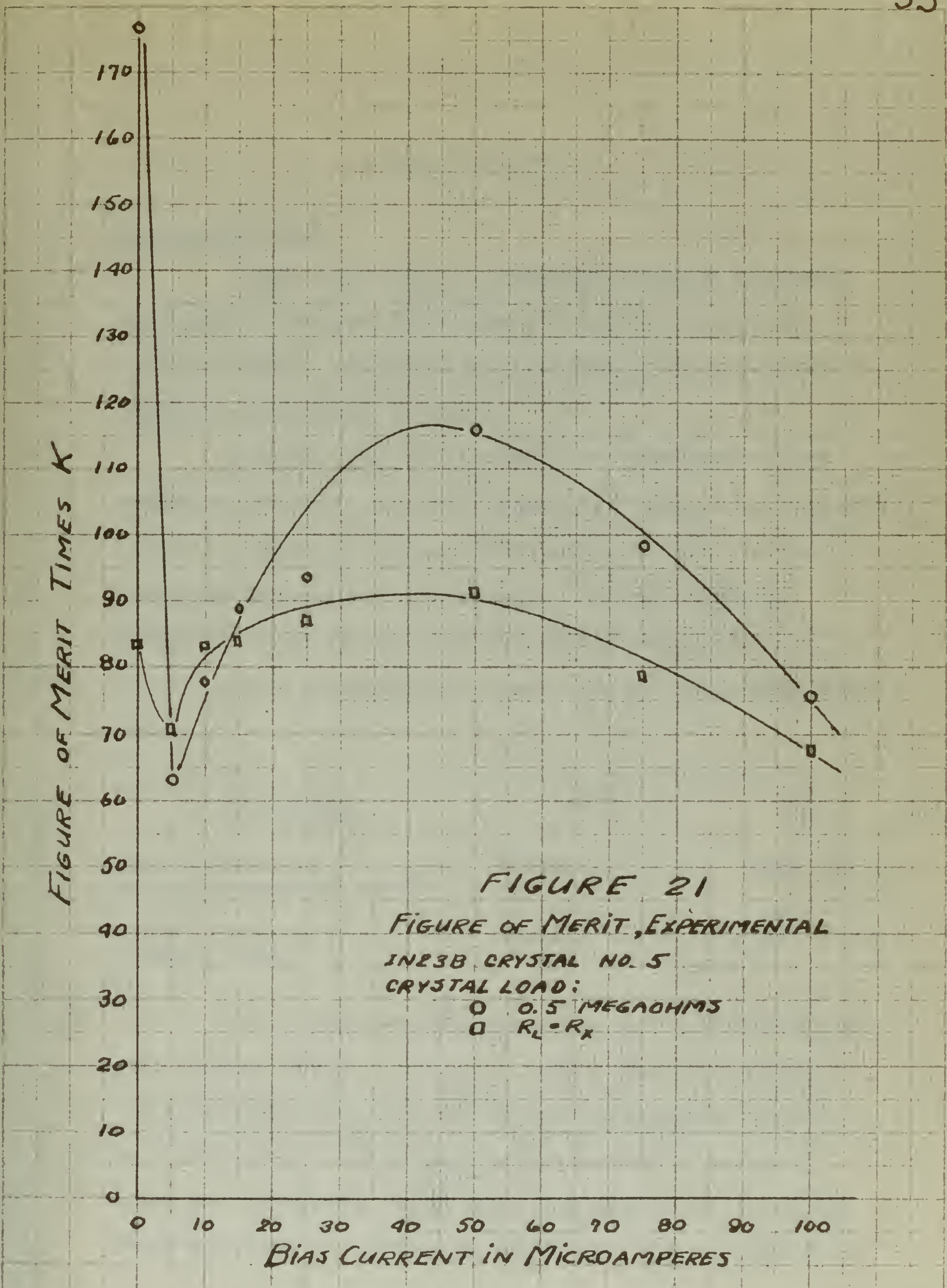

FIGURE 21

FIGURE OF MERIT, EXPERIMENTAL

1N23B CRYSTAL NO. 5

ANALYSIS OF RESULTS

Crystal Resistance

Figure 8 shows that the variation of crystal resistance is negligible for power input between 0.03 and 1.0 microwatts (45dbm to 30dbm). The results are considered to be valid within the microwatt region (50dbm to 20dbm).

Figures 9, 10, 11 and 12 give the variation of crystal resistance with bias. At 10 microamperes the value of the resistance obtained is about 3,000 ohms, and the results given by the two different methods are in good agreement. Crystal resistance determined by the two methods at 0.0 and 5.0 microamperes bias current are not in agreement as is shown by the average values given below.

Bias Current (microamperes)	0.0	5.0	
Crystal resistance (constant-power-line method)	15,000	6,000	(ohms)
Crystal resistance (halving method)	10,000	4,800	(ohms)

The constant-power-line-tangent method is believed to give more accurate results. In using the halving method, no allowance was made for the increase in the 60 cycle noise voltage developed by the crystal with the decrease in bias below 10 microamperes. Above 10.0 microamperes the 60 cycle noise voltage was negligible. Below this value the increase was of the same order of magnitude as

that of the increase in crystal resistance. It is believed that this 60 cycle noise voltage increase is a crystal phenomenon caused by the presence in the crystal holder of 60 cycle magnetic fields. Shielding of the equipment gave no noticeable change in the effect.

The shape of the curve in Figure 12 suggests a power-law variation of R_x as a function of bias. The nature of this variation is clearly seen by plotting the curves of Figure 12 on log-log paper as has been done in Figure 22. Since the slope of the curves is a constant above 10.0 microamperes,

$$\frac{\Delta(\log R_x)}{\Delta(\log I)} = -a \tag{14}$$

Taking the limit as ,

$$\frac{d(\log R_x)}{d(\log I)} = -a \tag{15}$$

Converting Equation 15 to natural logarithms and integrating,

$$\ln R_x = \ln I^{(-a)} + C \tag{16}$$

and

$$R_x I^{a} = C_1 \tag{17}$$

Below 10.0 microamperes bias current the exponent a is not a constant but is a function of the bias and Equation 17 takes the form

$$R_x I^{[a=f(I)]} = C_1 \tag{18}$$

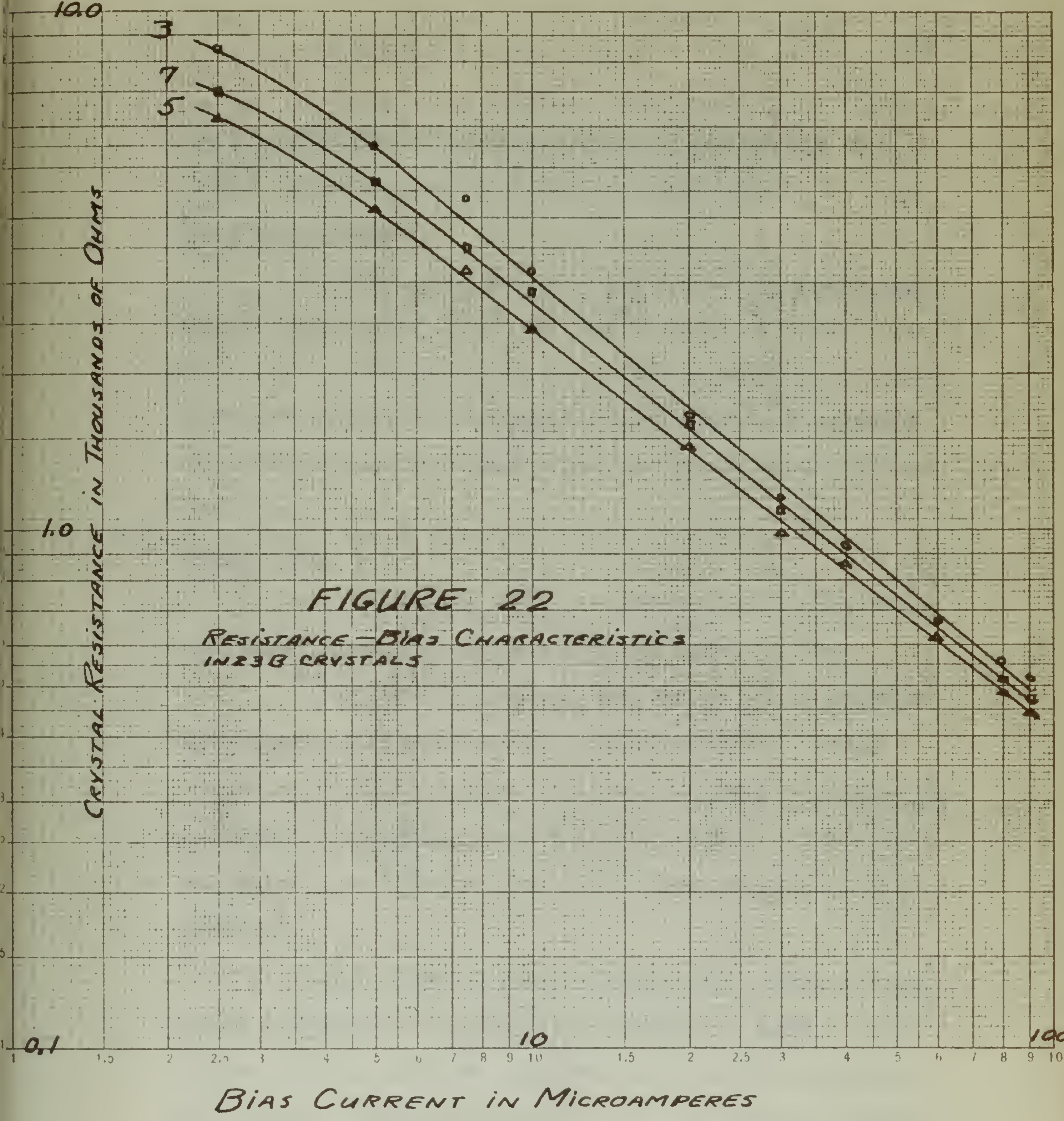

FIGURE 22

RESISTANCE—BIAS CHARACTERISTICS
IN23B CRYSTALS

From Equation 18 the crystal voltage-current characteristic equation may be written as

$$V_x I^{(1-a)} = C_1 \tag{19}$$

where the exponent a is constant above 10.0 microamperes bias current and a function of the bias below this value.

Current Sensitivity

Figure 13 shows that the curves of current sensitivity as a function of bias current of 1N23B crystals are parabolic in shape. For conditions studied, the maximum is reached for a bias current of about 80.0 microamperes. This result is in agreement with data taken on other types of crystals by Meyerhof, Serin and Vough (21).

Voltage Output

Crystal voltage output is a function of the load and the bias as the results of Figures 14, 15, 16 and 17 show.

From Figure 14 it is seen that as the load is increased the voltage output increases and the point of maximum voltage output moves toward zero bias. The locus of maximum voltage output is shown in the figures. From this it is possible to interpolate the optimum bias conditions for the load into which a crystal is operating.

Figures 15 and 16 show that the crystal voltage output varies critically in the negative bias region. A point of zero output is seen to exist at approximately minus 0.08 microamperes bias current. This zero output point is seen to be near the point

of inflection of the d-c characteristic curve given in Figure 3, an expanded view of the negative half of the curve being given in Figure 23. Close inspection of Figure 23 shows the inflection point to be at approximately minus 1.0 microamperes.

In Figure 17 the slope of the curves show that 1N23B crystals are very nearly square-law rectifiers within the region tested. For the 2,000 ohm load used the maximum voltage output condition is shown to be at 30 microamperes bias current. The 2,000 ohm load curve in Figures 14 and 24 show a maximum at approximately this same bias current.

To determine the validity of the above data for use with wide band amplifiers the TAA-16EA was replaced by a Ballantine voltmeter and decade amplifier, which had a band pass of from 30 cps to 300 Kcps, and the information presented in Figure 14 was repeated for this wide band case. The results are shown in Figure 24. Comparison of Figures 14 and 24 show that the results of the wide and narrow band cases are in agreement. The linear scale factor between the ordinates of the two sets of curves is due to the difference in amplifier gain.

From the above discussion it is seen that if the crystal output is to be voltage amplified, narrow or wide band, it is necessary that the crystal load be as large as possible, and that the bias be very near or equal to zero. If it is necessary to operate a crystal into a voltage amplifier whose input resistance is below 50,000 ohms it is advantageous to bias the crystal. Interpolation of the maximum voltage output curve in Figures 14 and 24 gives the necessary bias for the load to be used with the crystal.

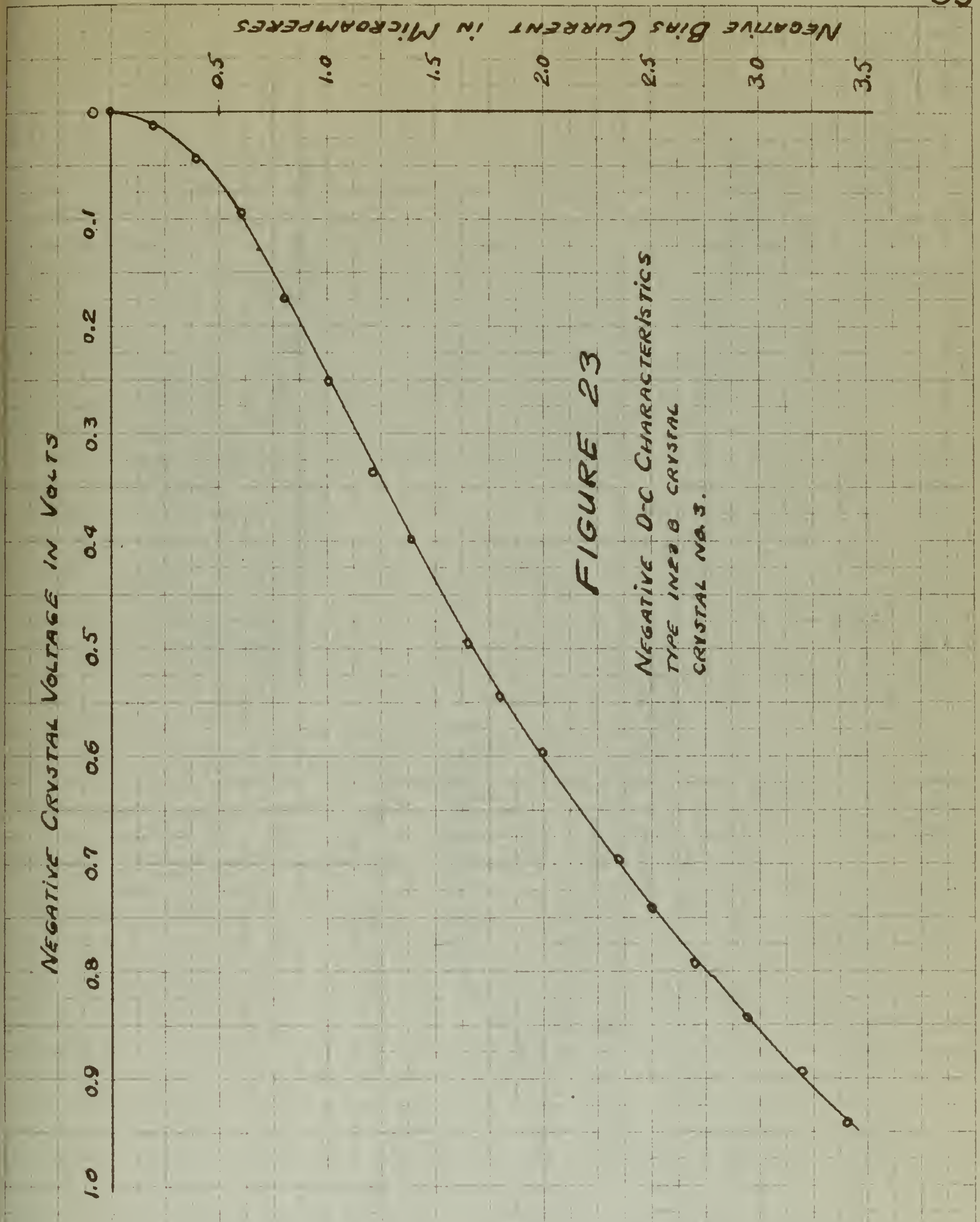

FIGURE 23

Negative D-C Characteristics
Type 1N23 B Crystal
Crystal No. 3.

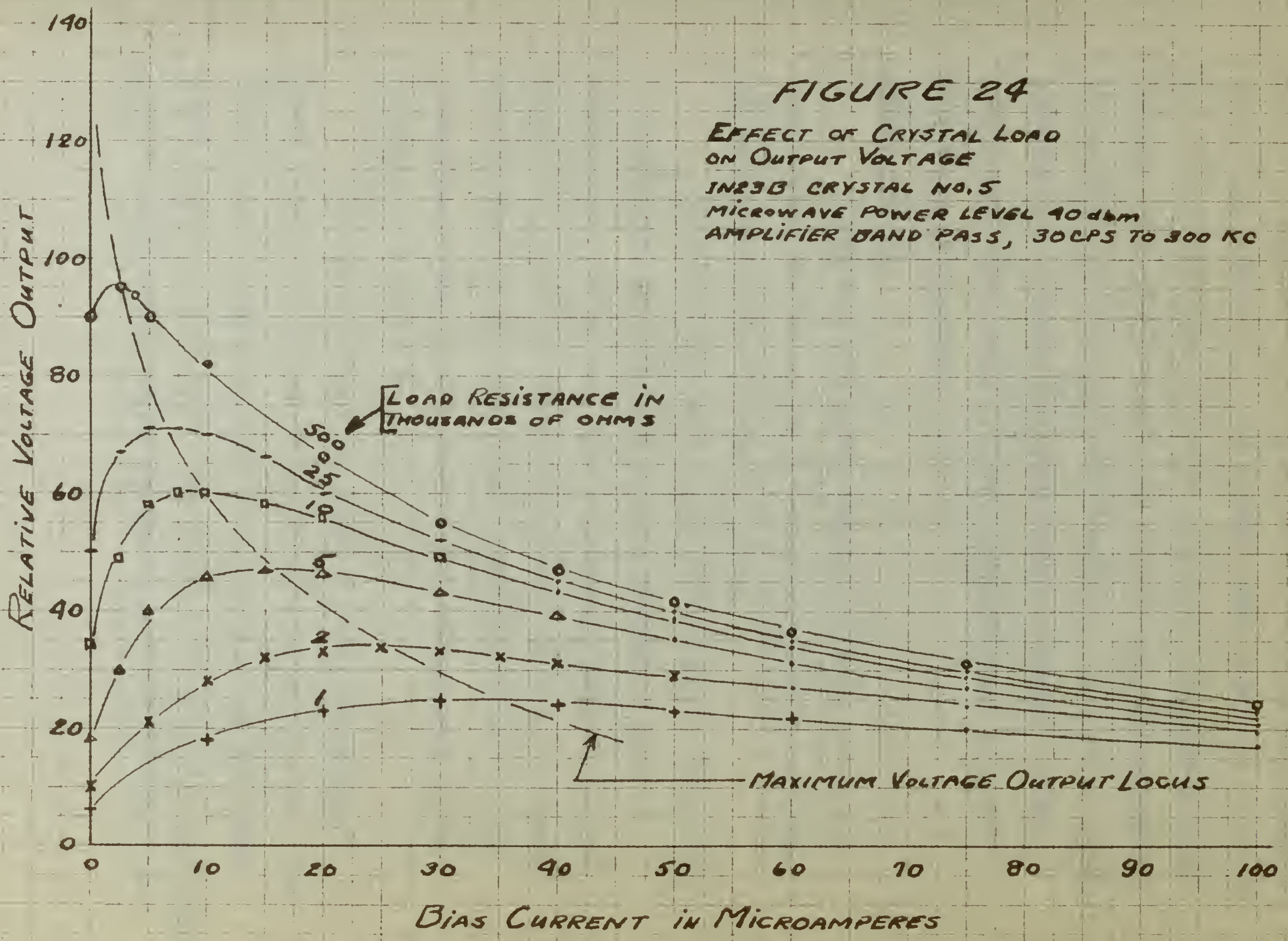

FIGURE 24

Effect of Crystal Load on Output Voltage

1N23B Crystal No. 5

Microwave Power Level 40 dbm

Amplifier Band Pass, 30 CPS to 300 KC

Output Power

Maximum output power is a function of the crystal bias as is shown in Figure 19. The maximum output power bias condition for all crystals tested is in the region of 30 microamperes bias current. It is of interest to note that at this bias the crystal will be operating at a near maximum signal-to-noise voltage output ratio as will be shown in the next section. The slope of the power output curves below 20 microamperes indicates that control of the bias is necessary.

Figure of Merit

There is a wide discrepancy in the Figure of Merit as determined by the two methods, computation from narrow band data and experimentally for the wide band case.

From the narrow band Figure of Merit curves (Figure 20) it is seen that best operation is to be obtained at about 20 microamperes bias current. This is reasonable since the current sensitivity curves show a similar increase. It is to be pointed out that there may have been present the effect of the 60 cycle noise voltage below 10 microamperes which could account for the large drop in M in this region.

In taking the data for Figure 21, care was taken to insure that the noise observed was not that due to 60 cycles. The 60 cycle noise voltage was nullified by superimposing the crystal output signal on the 60 cycle noise output and reading the superimposed signal-to-noise ratio. Though the zero bias condition shows a high

Figure of Merit the crystal should not be operated at this point unless the amplification unit is capable of rejecting the 60 cycle noise component and all its harmonics.

If the 60 cycle noise voltage can be eliminated then crystal rectifiers can be operated at zero bias in conjunction with voltage amplifiers to give excellent signal-to-noise voltage output characteristics. However, if the 60 cycle noise voltage can not be rejected in some manner then the crystal should be operated at about 50 microamperes bias current for best signal-to-noise voltage output ratio.

VI

CONCLUSIONS

The load on the IN23B crystal and the type of amplification unit it feeds determines the bias at which the crystal should be operated.

The data compiled in this paper is believed to be sufficiently accurate for use in design of units using IN23B crystals as low-level detectors.

Further work is indicated to determine the cause and effect of the 60 cycle noise voltage developed by the crystal in the zero to 10 microampere bias region.

BIBLIOGRAPHY

1 Cruft Electronics Staff, *Electronic Tubes and Circuits.* New York: McGraw-Hill Book Company, Inc., 1947, p 294.

2 Torrey, H. C., C. A. Whitmer, *Crystal Rectifiers.* New York: McGraw-Hill Book Company, Inc., 1948, 443 pp.

3 Angello, S. J., "Semiconductor Rectifiers," *Electrical Engineering* 68:865 Oct, 1949.

4 Bardeen, John, "Surface States of Rectification of a Metal-Semiconductor Contact," *Physical Review*, 71:717-27, May 15, 1947.

5 Bardeen, John, "On the Theory of the A-C Impedance of a Contact Rectifier," *Bell System Technical Journal*, XXVIII-3:428, July, 1949.

6 Bardeen, John, G. L. Pearson, "Electrical Properties of Pure Silicon and Silicon Alloys," *Physical Review*, 75:865-883, 1949.

7 Beringer, R., "Crystal Detectors and Crystal Video Receiver," *NDRC Report* 14-638, Nov 16, 1944.

8 Beth, H. A., "Theory of High Frequency Rectification by Silicon Crystals," *RL-NDRC Report* 14-184, Oct 29, 1942.

9 Brattain, W. H., J. Bardeen, "Nature of the Forward Current in Germanium Point Contacts, *Physical Review*, 74:238, 1948.

10 Conwell, E., V. F. Weisskopf, "Theory of Impurity Scattering in Semiconductors," *Physical Review*, 69:258, 1948.

11 Fan, H. Y., "Theory of Rectification of an Insulating Layer," Physical Review, Vol 74, Nov 15, 1948.

12 Herzfeld, K. F., "The Influence of Surface Conditions and Space Charges on the Conductivity of Poor Conductors," *Physical Review*, 34:791, 1949.

13 Joffee, J., "A Summary in English of Schottky's Papers on The Potential Distribution in the Transition Region," Electrical Communications, 22:217, 1949.

14 Lawson, A. W., et al, "Behavior of Silicon Crystals at Low Level Powers," University of Pennsylvania, *NDRC Report* 14-182, Sept 1, 1943.

15 Lawson, A. W., et al, "High Frequency Rectification Efficiency of Crystals," University of Pennsylvania, *NDRC Report* 14-153, July 1, 1943.

16 Lark-Horovitz, K., "Preparation of Semiconductors and Development of Crystal Rectifiers," *NDRC Report* 14-585, covering period from March 1942 to Nov 1945.

17 Lark-Horovitz, K., V. A. Johnson, "Theory of Resistivity in Germanium Alloys," *Physical Review*, 69:258, 1946.

18 Lark-Horovitz, K., "Conductivity in Semiconductors," *Electrical Engineering*, 68:1047, Dec 1949

19 Meyerhof, W. E., "Development Research on X Band Video Crystals," University of Pennsylvania *NDRC Report* 14-501, Sept 11, 1945.

20 Meyerhof, W. E., R. A. Stephens, "X Band Video Crystals," University of Pennsylvania, *NDRC Report* 14-274, May 20, 1944.

21 Meyerhof, et al, "X Band Crystal Performance With Bias," University of Pennsylvania, *NDRC Report* 14-505, July 6 1945.

22 Meyerhof, W. E., "Contact Potential in Silicon Crystal Rectifiers," *Physical Review*, Vol 17, May 15, 1947.

23 Miller, P. H., Jr., M. H. Greenblatt, "Crystal Audio Noise," University of Pennsylvania, *NDRC Report* 14-387, Jan 5, 1945.

24 Schaff, J. H., et al, "P-Type and N-Type Silicon," *Metals* Transactions, 185:383-388, 1949.

25 Smith, A. A., "Crystal Noise as a Function of D-C Bias and 30 mc Impedance Measured With a Diode Noise Source," Purdue University, *NDRC Report* 14-167, June 25, 1943.

26 Editorial Note Regarding Semiconductors, *The Bell System Technical Journal*, XXVIII-3:335, July, 1949.

27 "Symposium on Electrical Properties of Semiconductors and Transistors," Jan, 1950, (A series of four articles, compilations of papers originally presented at a Symposium on Electrical Properties of Semiconductors and The Transistor, held during the AIEE Summer General Meeting, Swampscott, Massachusetts, June 20-24, 1949.

VITA

The author was born in Bay City, Michigan, June 2, 1920. He received his Associate Bachelor of Science degree from the Bay City Junior College in 1939. In 1940, he entered the U. S. Naval Academy and graduated in 1943 with the degree of Bachelor of Science.

Since 1943, he has served as a commissioned officer in the U. S. Marine Corps.

In 1947, he was admitted to the U. S. Naval Postgraduate School, Department of Ordnance Engineering, and upon completion of the first year of a three year course was admitted to the Graduate School of Engineering, The Johns Hopkins University for completion of the course.

Thesis 13249
R895 Rushlow
An experimental determination of the low-level characteristics of IN23B crystals.